

**THE STRUCTURE OF THE TRANSVERSE CARPAL LIGAMENT: ITS COLLAGEN
FIBER ORIENTATION AND THE EFFICACY OF COLLAGENASE IN DECREASING
ITS STIFFNESS**

by

Ryan Prantil

B.S., Syracuse University, 2008

Submitted to the Graduate Faculty of
Swanson School of Engineering in partial fulfillment
of the requirements for the degree of
Master of Science in Bioengineering

University of Pittsburgh

2011

UNIVERSITY OF PITTSBURGH
SWANSON SCHOOL OF ENGINEERING

This thesis was presented

by

Ryan Prantil

It was defended on

July 12, 2011

and approved by

Savio L-Y. Woo, Ph.D., D.Sc., D.Eng.
Departments of Bioengineering, Mechanical Engineering, and Rehabilitation Science &
Technology

Steven D. Abramowitch, Ph.D.
Departments of Bioengineering and Obstetrics, Gynecology, and Reproductive Sciences

Thesis Advisor: Zong-Ming Li, Ph.D., Cleveland Clinic
Departments of Biomedical Engineering, Orthopedic Surgery, and Physical Medicine &
Rehabilitation

Copyright © by Ryan Prantil

2011

THE STRUCTURE OF THE TRANSVERSE CARPAL LIGAMENT: ITS COLLAGEN FIBER ORIENTATION AND THE EFFICACY OF COLLAGENASE IN DECREASING ITS STIFFNESS

Ryan Prantil, M.S.

University of Pittsburgh, 2011

Carpal tunnel syndrome (CTS) currently affects more than three million Americans each year. Hand surgeons treat CTS by targeting the transverse carpal ligament (TCL) which acts as the palmar roof of the carpal tunnel. Based on general observation, the TCL appears to be an inextensible collagenous matrix with fibers roughly oriented along the transverse direction. Several studies on the TCL's configuration argue for different fiber orientations consisting of either oblique or transverse orientations; whereas, most findings were based on an observational methodology. Very few studies have determined such fiber orientations; whereas, even fewer studies have researched the ligament's mechanical properties. Furthermore, the potential of altering the TCL's microstructure may provide a potential, alternative to the currently accepted, invasive standards.

Previous studies attempting to lengthen the TCL found that such procedures can effectively diminish CTS symptoms and also decrease the progression of several post-operative complications. However, these procedures consist of transecting the transverse carpal ligament in an attempt to increase its length. Furthermore, mechanical stimuli cannot alter the ligament because it is too stiff. In addition, such procedures also require invasive surgery and can cause complications that arise from carpal tunnel release. Therefore, a solution might lie in the application of collagenase where antecedent works have shown its capacity to reduce the mechanical properties of a tissue.

The following studies have emphasized the transverse carpal ligament's collagen orientation and its mechanical response to subsequent collagenase treatment. The preferential collagen direction was quantified through the use of small angle light scattering (SALS). Results showed that transverse orientation was the most prevalent with minimal changes found within its orientation along its thickness. As for the TCL's response to collagenase, standard concentrations of collagenase were applied to the TCL for each specimen through successive mechanical loading protocols along with successive observations to analyze the progressive changes within the ligament by slowly eliminating its collagen network. Collagenase effectively decreased the transverse carpal ligament's stiffness without significantly changing its mechanical properties. Furthermore, these studies could contribute to a more sophisticated model of the TCL and lead to the development of a minimally invasive therapy contrary to current, invasive standards.

DESCRIPTORS

Carpal Tunnel Mechanics

Collagen Fiber Orientation

Carpal Tunnel Syndrome

Small Angle Light Scattering

Collagenase

Transverse Carpal Ligament

TABLE OF CONTENTS

ABSTRACT	IV
DESCRIPTORS	V
LIST OF TABLES	X
LIST OF FIGURES	XI
ABBREVIATIONS	XV
ACKNOWLEDGMENTS	XVII
1.0 INTRODUCTION	1
1.1 MOTIVATION	1
1.2 CARPAL TUNNEL ANATOMY	1
1.3 CARPAL TUNNEL SYNDROME	3
1.4 TCL FUNCTION AND CTR COMPLICATIONS	5
1.5 ALTERNATIVE THERAPIES FOR CTS	7
2.0 SPECIFIC AIMS	10
2.1 AIM 1.....	10
2.2 AIM 2.....	11
3.0 FIBER ORIENTATION OF THE TCL	14
3.1 OBSERVATIONS OF TCL FIBER ORIENTATION	14
3.2 SMALL ANGLE LIGHT SCATTERING	15
3.3 TCL FIBER QUANTIFICATION	17
3.3.1 Experimental preparation	17
3.3.2 Imaging preparation	18

3.3.3 Data processing	19
3.4 RESULTS	21
3.4.1 Laminar changes within fiber orientation	21
3.4.2 Fiber percentages	23
3.5 DISCUSSION	24
3.5.1 The collagen fiber orientation of the TCL	24
3.5.2 Future model implementation	26
4.0 INITIAL OBSERVATIONS OF COLLAGENOLYTIC EFFECTS	27
4.1 THE BIOLOGY OF COLLAGENASE DEGRADATION	27
4.2 OBSERVATION PROCEDURE	30
4.3 RESULTS	31
4.4 DISCUSSION	33
5.0 COLLAGENASE’S EFFECTS ON TCL MECHANICS: PRELIMINARY STUDIES	35
5.1 THE EFFECT OF COLLAGENASE ON TISSUE MECHANICS	35
5.1.1 Effects on elasticity	35
5.1.2 Effects on viscoelasticity	37
5.2 EXPERIMENT 1: STRAINED TO FAILURE	39

5.2.1 Methodology.....	39
5.2.1a Testing protocol	39
5.2.1b Data analysis	41
5.2.2 Results	43
5.2.2a Stress-strain curves	43
5.2.2b Mechanical properties	44
5.3 EXPERIMENT 2: SUBMAXIMAL TESTING	48
5.3.1 Adjustments	48
5.3.1a Repeated measures design.....	48
5.3.1b Sub-maximal testing protocol.....	49
5.3.2 Results	50
5.4 EXPERIMENT 3: TESTING AT ROOM TEMPERATURE	51
5.4.1 Adjustments	51
5.4.1a Collagenase preparation	51
5.4.1b Parameter estimation	52
5.4.2 Results	52
5.5 DISCUSSION	58

5.5.1 Experiment 1	58
5.5.2 Experiment 2	59
5.5.3 Experiment 3	60
6.0 COLLAGENOLYTIC CHANGES TO THE TCL'S TENSILE PROPERTIES	61
6.1 VARIABLES AFFECTING COLLAGENASE	61
6.2 EXPERIMENTAL DESIGN: ADJUSTMENTS	63
6.3 RESULTS	64
6.4 DISCUSSION	68
6.4.1 Collagenase activity	68
6.4.2 Future studies	70
7.0 CONCLUSION	72
BIBLIOGRAPHY	75

LIST OF TABLES

Table 1.1.	Shows the effect of various types of TCL lengthening and their respective effect on carpal tunnel volume. Columns represent values of interest: (1) Technique, (2) Pre-operative carpal tunnel volume (Average \pm Std. Dev.), (3) Post-operative carpal tunnel volume (Average \pm Std. Dev.), (4) Percent Increase in carpal tunnel volume, (6) Statistical significance (Modified from Pavlidis et al. 2010)9
Table 4.1.	The measured activity of various types of collagenases from different commercial sources where each column signified a measure of importance with regards to collagenolytic activity: (1) Supplier, (2) Designation, (3) Lot Number, (4) Ratio of protein, (5) Several measures of specific activity (Bond MD 1984, Document Source: Bhavya 2006)29
Table 4.2.	Shows the written observation of subsequent changes to respective ligaments with the addition of several concentrations of collagenase where physical and visual efforts were made to document collagenolytic activity32
Table 6.1.	Failure points (\times) of each sample are tabulated with respect to at what point during the testing protocol and after which time duration of treatment65

LIST OF FIGURES

Figure 1.1.	This figure outlines the anatomy of the transverse carpal ligament and its bone insertion sites as well as other features. Please note that this is an idealization where other soft tissue structures do attach to the TCL.....	3
Figure 1.2.	Shown is the TCL transected which allows for symptoms associated with carpal tunnel syndrome to subside	4
Figure 1.3.	This is an idealistic overview of the progression of post-operative complications where TCL transection causes significant changes within the patient’s carpal tunnel anatomy	6
Figure 1.4.	An overview of several TCL reconstruction methods that aim to increase the length of the TCL and reduce the risk of post-operative complications. These lengthening techniques were research and used in the following studies: (a) Netscher et al., 1998, (b) Jakab et al., 1991, (c) Sennwald 1987, and (d) Pavlidis et al., 2010. ⁽¹⁾	9
Figure 2.1.	MMP1 interaction with type 1 collagen is diagrammed in this figure. Type 1 collagen forms a triple helix with alpha-1 chains and an alpha-2 chain. (Left) Shows the domains of MMP1 and the triple helical structure while (Right) this enzyme forms charges causing attraction/repulsion forces which form the basis of collagen disassociation. ⁽²⁾	12
Figure 3.1.	The laminar configurations of TCL are shown along with their respective prominence that was measured within Isogai et al where type 1, type 2, type 3 and type 4 configurations are distinguished by their respective fiber orientations within their superficial and deep layers. ⁽³⁾	15
Figure 3.2.	Experimental setup for SALS is shown where the flow of information is dictated by angles at which the refraction of the laser beam are shone on the ground glass screen (adapted from Sacks et al.). ⁽⁴⁾	16
Figure 3.3.	Shows how fibers were designated with regards to their angle of orientations where respective fiber orientation separated within the following regions: the transverse, pisiform-trapezium (PT Oblique), longitudinal, and scaphoid-hamate (SH Oblique) directions	20

Figure 3.4.	This figure reveals the SALS outputs for the various depths of a respective specimen (a) 25% depth, (b) 50% depth, and (c) 75% depth (0%: volar side of TCL).75% depths (0%: volar side of TCL)	22
Figure 3.5.	Average histograms were computed for preferred fiber directions and are shown in this figure where designated axes are also revealed which represents the aforementioned divided areas of orientation. TCL levels of interest are the following: (a) 25%, (b) 50%, and (c) 75%.....	23
Figure 3.6.	Fiber percentages for orientations of interest are shown for each TCL level of interest (25%, 50%, and 75%). All of which was measured with respect to reference depth of 0% or the volar side of TCL	24
Figure 4.1.	This figures shows the general anatomy of various dorsal wrist ligaments where (4) is designated for the dorsal intercarpal ligament while (5) is designated for a portion of the dorsal carpal ligament which is located just superficial to the dorsal intercarpal ligament, respectively. Both ligaments were used in the observation study where the extensor retinaculum isn't shown within the figure but was also included (Source: Goldfarb et al. 2001). ⁽⁵⁾	31
Figure 4.2.	The visual changes caused by collagenase are shown in the series of pictures where each ligament segment is shown before and after each hour of treatment	33
Figure 5.1.	The stress vs. strain curves of comparing control pathogenic chords (□) to treated chords which utilized 3600 U (◇) of collagenase for 24 hours. This figure was taken from Starkweather et al. ⁽⁶⁾	36
Figure 5.2.	The stress vs. strain curves comparing control and various collagenase-treated periodontal ligaments for 4 hours; whereas, the concentrations of collagenase are shown at the bottom: control (○), 8 U (●), 16 U (Δ), and 24 U (▲). This figure taken from Kawada et al. ⁽⁷⁾	37
Figure 5.3.	Outlines the stress-relaxation curves comparing control (○) and treated (●) periodontal ligaments where the ligament was treated with 8 units of collagenase per milliliter of phosphate buffered saline. This figure was taken from Komatsu et al. ⁽⁸⁾	38
Figure 5.4.	Reveals the (a) grip positioning for each ligament sample as well as the respective sample's positioning to the (b) MTS apparatus	40

Figure 5.5.	Shows the representative testing protocol used for each ligament sample where the each sample was strained until failure. The top figure shows protocol in terms of displacement versus time while the bottom figure reveals the force versus time for the same testing protocol41
Figure 5.6.	Displays stress-strain curves of the various treated samples of three transverse carpal ligaments: control (○), 500 U (▲), 750 U (×, dark grey), 1000 U (✱, light grey), and 1250 U (◇). Those curves were separated in the following TCL specimen: (a) an unknown left hand, (b) an unknown right hand, and (c) a right hand44
Figure 5.7.	Shows the average tangent modulus with respect treatment duration where the statistics were computed across the three samples to test the effect of collagenase concentration45
Figure 5.8.	Shows the average stiffness (N/mm) trend with regards to the concentration of collagenase46
Figure 5.9.	Reveals the trend between average ultimate strain and the concentration of collagenase47
Figure 5.10.	Average values for ultimate stress are shown with regards to different concentrations of collagenase and the respective control group47
Figure 5.11.	Shows the sub-maximal testing protocol that was utilized for the preconditioning and testing phases in mechanically testing each ligament sample49
Figure 5.12.	Stiffness results are shown for both the control and the treated proximal segment on the left end as opposed to the control and the treated distal segment which is positioned on the right end of the graph50
Figure 5.13.	The results for tangent modulus are revealed with the control and the treated proximal segment positioned on the left end of the graph while the control and the treated distal segment are positioned on the right end of the graph.51
Figure 5.14.	Highlights the general process used to analyze the mechanical properties for each ligament sample: (Step-1) Determine region for force versus displacement graph, (Step-2) Pick region for stiffness analysis, and (Step-3) Pick region for tangent modulus analysis.....53

Figure 5.15.	Displayed in this figure is the average thickness estimate for each TCL sample measured with the LVDT before collagenase treatment and after each hour of treatment	54
Figure 5.16.	Shown in this diagram is the average stiffness calculated among the tested TCL samples before collagenase treatment and after each hour of treatment	55
Figure 5.17.	Depicted in this diagram is the trend between the average tangent modulus and collagenase treatment duration	56
Figure 5.18.	Outlines the relationship between maximum strain and collagenase treatment duration where testing was sub-maximal with a load limit of 5 N	57
Figure 5.19.	Displayed in this picture are the microscope pictures that were taken for the ligament sample after 1-hour, 2-hour, 3-hour, and 4-hour of treatments. Please note that control pictures weren't taken	58
Figure 6.1.	Representative displacement-force curves of a sample show the repeated measures for before treatment and after the first hour, second hour, and third hour of treatments	65
Figure 6.2.	Average stiffness is shown in the repeated measures design for the control measurements and after the first hour, second hour, and third hour of treatments	66
Figure 6.3.	Tangent modulus is shown within this figure with regards to the samples' measurements for control and after different, treatment durations	67
Figure 6.4.	Shown for this figure are the common visual changes that are seen within the second TCL sample before and after a treatment of three hours	68

ABBREVIATIONS

$^{14}\text{CH}_3$: Collagen or Casein

ANOVA: Analysis of Variance

BAEE: N- α -Benzoyl-L-Arginine Ethylester

CDU: Collagenase Digested Units

CSA: Cross-Sectional Area

CTBP: Carpal Tunnel Balloon Plasty

CTR: Carpal Tunnel Release

CTS: Carpal Tunnel Syndrome

DC: Dupuytren's Contracture

FALGPA: Synthetic Polypeptide 2-Furanacryloyl-L-Leucylglycyl-L-Prolyl-L-Alanine

HBSS: Hank's Balanced Salt Solution

HeNe: Helium Neon

LVDT: Linear-Variable Differential Transducer

MMP1: Matrix Metalloproteinase 1

nkat: Nanoketals (Nanomoles per second)

OI: Orientation Index

PBS: Phosphate Buffered Saline

PT: Pisiform Trapezium

SALS: Small Angle Light Scattering

SSCT: Sub-Synovial Connective Tissue

SH: Scaphoid Hamate

TCL: Transverse Carpal Ligament

U: Units of Collagenase

ACKNOWLEDGMENTS

In 2008, young, naïve, and unconfident, I entered graduate school to accomplish my goal in life. I needed motivation and determination to pursue my future work. Fortunately, I found people to support my endeavors. I greatly appreciate the people within and outside the University of Pittsburgh. They were very supportive and inspirational.

First, I would like to mention my family. The life lessons which were taught to me continue to be the main reasons why I chose Bioengineering and why I continue to look for further advancement within the field. I am forever indebted to them for their consideration and love.

In addition, I must recognize Gustav Engbretson, Ph.D., from Syracuse University for the beginning of my educational journey in the field of Bioengineering. His guidance and expertise have had such a great impact on my life as a future scientist and engineer.

Second, I have had the great pleasure to work with a great mentor in Dr. Zong-Ming Li both in Pittsburgh and in Cleveland. His employees were and are exceptionally coordinated as well as organized; and without their help and their tutelage, I would not have completed my experimental work or thesis. Therefore, I would also like to extend this acknowledgement to Tracy, Juno, Mat, Tamara, Joe, Ian, Julie, Ana and many others. Although I had several problems with my research, Dr. Li provided me not only with wonderful advice concerning my research but he also often provided me with encouragement to finish. His tutelage and consideration will always be cherished. And to this day, I look to him not only as a research advisor but also as a friend.

Third, I wish to thank Kaihua Xiu. Both her experience and knowledge on the carpal tunnel, imaging, and soft tissue mechanics have made my transition easier and have helped me to carry out these studies that I shall address. She assisted and answered all of my questions, and I am forever thankful for her efforts and consideration in my studies. Additionally, I would also like to acknowledge Xiu Guo, Hong Pan, and Hana Fayaz for their respective efforts in refining my experimental attempts in answering different research questions.

Fourth, I would like to thank the MSRC for their support in accommodating me when Dr. Li moved to Cleveland. I continuously look up to Dr. Woo as not only a great researcher, but also as a great human being. His help and consideration, his employees, and his students have proven paramount to all of my research successes and my thesis completion. His ACL group has performed as a perfect working model in addressing current clinical problems. Kwang Kim, Dr. Rui Liang, Dr. Huinan Liu and Matthew Fisher have helped me considerably in refining and in answering my various research questions.

Fifth, I wish to thank Dr. Steven Abramowitch. His wonderful expertise and excellent advice were invaluable to my efforts in this endeavor. In the past, I can remember the advice that he gave me when I wasn't successful as an undergraduate student during my internship at the MSRC. He told me not to worry and that such failures are a part of research. Those words not only helped me to finish but they will also help me to continue in the future. I will always be grateful for his superior mentorship.

Finally, I would like to thank the Bioengineering faculty for their assistance and tutelage. I have had the great privilege to learn among several of the great minds within the Bioengineering department, and I am forever indebted for their help and teaching. In all, I wish to thank everyone within the department. This has been an experience that I shall always cherish and look upon fondly.

1.0 INTRODUCTION

1.1 MOTIVATION

Cadaveric and in-vivo studies prove to be taxing in both time and money for all research endeavors. Those aforementioned problems have caused many researchers to turn to the use of accurate simulation through computational advances. Current research on wrist biomechanical finite element simulations has been limited to both distal radius and scaphoid fracture⁽⁹⁻¹²⁾; whereas, even fewer models address the impending post-operative complications resulting from carpal tunnel release.⁽¹³⁾ However, past analyses of different soft tissue structures must consider collagen fiber orientation as well as its associated dispersion; whereas, such orientation might also provide subsequent insights into a soft tissue's material perspective.^(14, 15) In contrast, current simulations of carpal tunnel release have made considerable idealizations for fiber orientation.⁽¹³⁾ In addition, past studies have indicated the TCL's essence for carpal tunnel biomechanics; thus, instead of its elimination, the modification of its collagen network could possibly alleviate the complications associated with carpal tunnel release.

1.2 CARPAL TUNNEL ANATOMY

The carpal tunnel encases tendons and the median nerve which run proximal-distally.⁽¹⁶⁾ Its medial, lateral, and posterior borders are formed by carpal bones and respective inter-carpal ligaments.⁽¹⁶⁾ In contrast, the palmar border of the carpal tunnel is produced by the transverse carpal ligament which is a sub-tissue of the flexor retinaculum.⁽¹⁷⁾ The flexor retinaculum is divided proximal-distally into three layers: antebrachial fascia, transverse carpal ligament, and the aponeurosis.⁽¹⁷⁾ Superficial to the antebrachial fascia is the a superficial fascial layer which

is just anterior to the median nerve and is continuous to the transverse carpal ligament where it is known as the proximal third of the flexor retinaculum. ⁽¹⁷⁾ The distal third is the aponeurosis of the thenar and hypothenar muscles where it is differentiated from other proximal tissues by a layer of adipose tissue. ⁽¹⁷⁾

The transverse carpal ligament (TCL) represents the middle-third of the flexor retinaculum where it forms the palmar roof of the carpal tunnel. However, recent studies have proposed to abandon the term of flexor retinaculum and its use in conjunction with the TCL. ⁽¹⁸⁾ All carpal tunnel contents consist of a total of nine extrinsic flexor tendons and the median nerve. The nine flexor tendons consist of the flexor digitorum profundus tendons, the digitorum superficialis tendons, and the flexor pollicis longus tendon. These tendons as well as the median nerve are loosely connected in the carpal tunnel by sub-synovial connective tissue (SSCT). ⁽¹⁹⁾ A flexor tendon-pulley is formed in conjunction with the transverse carpal ligament and the flexor tendon. ⁽²⁰⁾ Proximal attachments of the TCL are formed on the tubercle of the scaphoid and on the pisiform while distal insertions are found on the ridge of the trapezium and the hook of the hamate (Fig. 1.1). ⁽¹⁶⁾

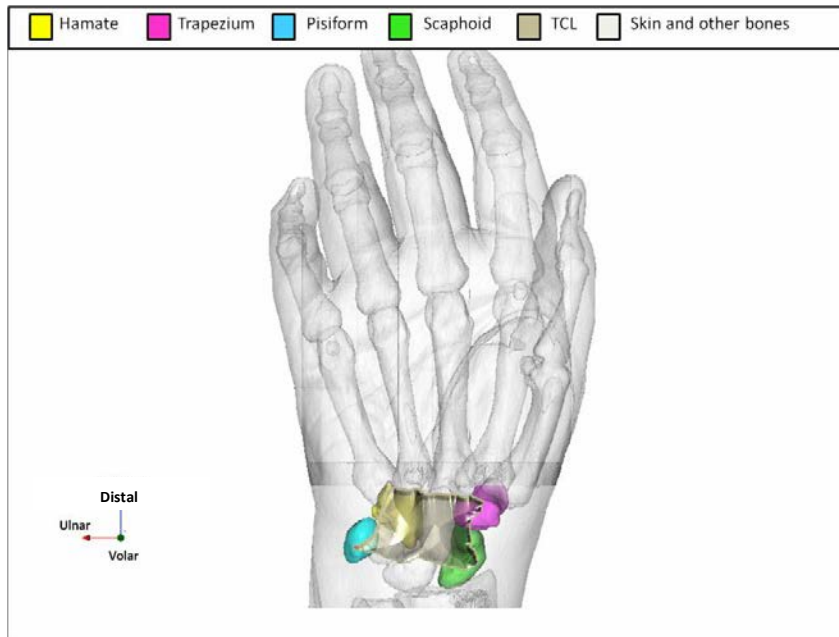


Figure 1.1. Highlights pertinent anatomy of the transverse carpal ligament.

1.3 CARPAL TUNNEL SYNDROME

Currently, CTS approximately affects three million Americans annually. ⁽²⁰⁾ CTS is classified as a compression neuropathy, in which the median nerve becomes impinged and causes reoccurring pain to the thumb, index, and middle fingers. ⁽²⁰⁾ Surgeons traditionally transect the TCL to release pressure from the median nerve to eliminate CTS symptoms. This type of procedure is commonly known as carpal tunnel release and consists of several variations (CTR) (Fig. 1.2).



Figure 1.2. Displays the critical soft tissue anatomy associated with CTS (Source: www.davisandderosa.com).

Several variations of TCL excision exist, but only two procedures are predominantly used: open release and endoscopic release. ⁽²⁰⁾ Both procedures are invasive; whereas, endoscopic release aims to preserve tissues overlying the carpal tunnel while open release divides such tissues with the intent of restoring their stability after TCL transection. ^(21, 22) Contrary studies are found in determining an optimal procedure with the fewest post-operative complications. ⁽²³⁾ Therefore, a gold standard has yet to be found due to separate groups of surgeons supporting either methodology. Ideal surgery characteristics of open release include its short operation time and low complication rate. ⁽²³⁾ Negative post-operative complications pertain to its induced lingering scar tenderness and weakening grip strength. ⁽²³⁾ Open release's counterpart, endoscopic release, was spawned in an attempt to alleviate the post-operative complications created by the original operation. Several variations of the procedure were created with several cases resulting in fewer instances of scar tenderness and reductions in recuperation time. ⁽²¹⁾ Disadvantages for this procedure stem from complications of incomplete release to associated cost increases in time and money with the addition of endoscopy. ⁽²⁰⁾ Both types of surgery have shown to be effective in relieving symptoms, regardless of the degree of invasiveness. ^(22, 24) However, extensive research has revealed that such measures could result in several post-operative complications associated with carpal tunnel biomechanics and anatomy. ^(22, 25)

1.4 TCL FUNCTION AND CTR COMPLICATIONS

As stated before (1.2), the TCL forms a pulley that anchors flexor tendons.⁽²⁶⁾ Additional studies have provided contrasting point-of-views concerning the TCL's impact on carpal tunnel stability.^(25, 27) Initially, Garcia-Elias et al. concluded that the TCL has minor effects on carpal tunnel stability.⁽²⁵⁾ However, several researchers have revisited such results by comparing it to their data and determined that the TCL's impact on stability is directionally dependent.⁽²⁷⁾ The original study ran tests in the dorsopalmar direction which revealed large discrepancies compared to recent compliance tests utilizing applied outward forces on TCL attachment sites.^(25, 27) Therefore, although its significance was originally deemed minor, updated research on the TCL's effect on carpal tunnel mechanics was found quite substantial, and its loss of function may lead to the development of several post-operative complications in addition to the situated tendons losing their anchor site.⁽²⁷⁾ Such research has validated the possible progression of several post-operative effects resulting from either variation of CTR.

Loss of the TCL function causes complications which further surmise due to the progression of several biomechanical and anatomical changes.⁽²⁰⁾ One of the most frequent complications is pillar pain which is frequently reported after either endoscopic or open release surgeries.^(28, 29) Associated changes in the carpal tunnel volume and carpal arch width may be responsible for the onset of pillar pain (Fig. 1.3).⁽²⁷⁾

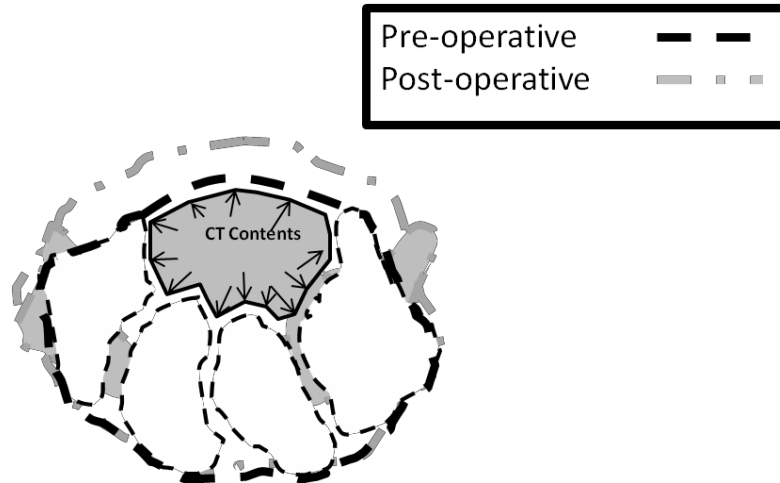


Figure 1.3. Changes in carpal bone articulation facilitate the progression of changes within the carpal tunnel.

Such anatomical changes may arise within the alteration developed within the intercarpal articulations of a post-CTR patient. Hand surgeons have characterized additional post-operative pain or tenderness associated with the thenar or hypothenar eminence; such pain may subside by the third month. However, the most common pain has been shown to originate in the pisotriquetral joint's articulation where the joint's dynamics become altered with the loss of TCL function.⁽³⁰⁾ Several potential etiologies for pillar pain are frequented: muscular or ligamentous and neurogenic. Muscular causes might be related to the intrinsic muscles of pinch and opposition relaxing with the severing of the TCL and the ensuing migration of the TCL to its boney origins.⁽³¹⁾ Neurogenic causes might possibly exist because subcutaneous tissue could be injured when incising in the "critical pillar rectangle" during open release surgery.⁽³²⁾ However, preemptive solutions do not exist for these causes, and further biomechanical changes within the carpal tunnel might ensue.

The TCL serves the three following functions: anchor the thenar and hypothenar muscles, stabilize the carpus in the transverse direction, and act as a pulley for flexor tendons. ^(26, 27, 33) Thus, the sectioning of the TCL negates these three functions and contributes to the aforementioned postoperative complications of pillar pain and grip weakness. Additional studies have focused on muscle anatomy and function in response to CTR. These studies revealed that certain muscles within the hand (flexor pollicis brevis, abductor pollicis brevis, opponens pollicis, and opponens digiti minimi) tend to shorten and lead to losses in muscle length as well as losses in muscle strength. ⁽³⁴⁾ Additional complications were also found within carpal bone articulation where piso-triquetral tracking and alignment become disrupted and result in significant pain. ⁽³⁰⁾ Further complications progress within the carpal tunnel as its contents tend to travel palmarward. ⁽²⁶⁾ Therefore, alternative therapies should be spawned in an attempt to eliminate such post-operative complications.

1.5 ALTERNATIVE THERAPIES FOR CTS

Substitute treatments vary from conservative therapy to similar all-invasive therapies. Current conservative treatments consist of steroid injection, ultrasound treatment, pyridoxine, oral medication, and various alternative invasive treatments, in which all modalities have been proven to be somewhat effective or not in use for immediate or long term treatment care. Non-steroidal anti-inflammatory medication and ibuprofen have been shown in the past literature to be non-effective for treating CTS. Similarly, pyridoxine has been suggested as a treatment; however, studies have failed to demonstrate its efficacy. ⁽³⁵⁾ Ultrasound treatment has been shown to have biophysical effects, such as nerve regeneration, on the median nerve. ⁽³⁶⁾ Ebenbichler has shown that ultrasound treatment can offer temporary relief for CTS patients; however, findings haven't been compared to other conservative and invasive therapies. ⁽³⁷⁾ Past studies also found success with the implementation of both steroid injection and casts targeting the distal edge of the carpal tunnel.

Median nerve compression has been determined to be distally located within the carpal tunnel. Research emphasize that the narrowest portion of the carpal tunnel which is located between the ridge of the trapezium and at the hook of the hamate, especially when the wrist is flexed. ⁽³⁸⁾ Carpal bone manipulation is utilized in an attempt to increase the distal cross-sectional area (CSA) at the aforementioned location. ⁽³⁹⁾ Such manipulation tends to rotate carpal bones and allows for subsequent increases in CSA, which would potentially decompress the median nerve. ⁽³⁹⁾ However, this treatment is in its infancy and has yet to be thoroughly researched where Li et al. are devoting much effort in utilizing such carpal bone motion to effectively treat carpal tunnel syndrome. ^(27, 39)

Additional invasive therapies have shown to be variably effective. Promising research has also been displayed in TCL reconstruction after excision which has the capacity to effectively increase carpal tunnel volume with the advent of lengthening the ligament. ⁽¹⁾ Several types of lengthening have shown significant increases to at least 31% within carpal tunnel volume (Table 1.1). ^(1, 40, 41)

Table 1.1. Shows the effect of TCL lengthening on carpal tunnel volume (Modified from Pavlidis et al. 2010).⁽¹⁾

Carpal tunnel volume changes from various types of TCL lengthening

Surgical Technique	Preoperative carpal tunnel volume (cm ³)	Postoperative carpal tunnel volume (cm ³)	Increase (%)	P-Value
Type A (Netscher et al., 1998)	4.6±1.64	6.6±1.97	44	<0.001
Type B (Jakab et al., 1991)	5.8±1.25	7.8±1.7	35	<0.001
Type C (Sennwald 1987)	5.95±0.85	8.1±1.3	36	<0.001
Type D (Pavlidis et al., 2010)	6.37±0.54	8.3±0.75	31	<0.001

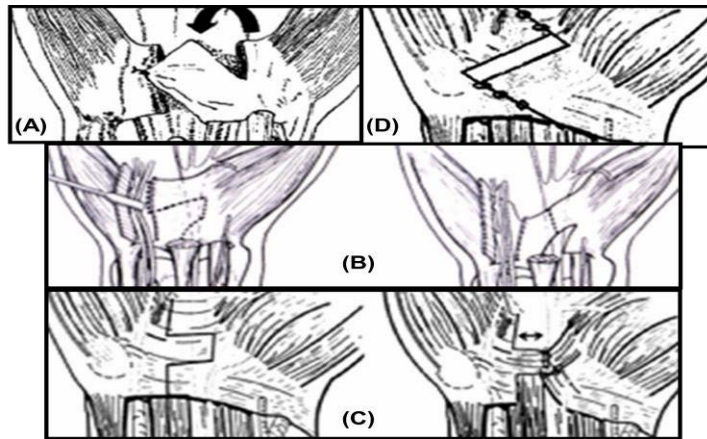


Figure 1.4. TCL lengthening techniques described in (1).

However, TCL reconstruction has been indicated as the only viable option for TCL lengthening. In contrast, the ligament has demonstrated to be too stiff to alter physically with load application.⁽³⁹⁾ Thus, TCL excision and reconstruction have to be employed; thereby, this process may subject a patient to several complications in order to release and reattach the ligament. Followed by subsequent force applications, alternative solutions could possibly incorporate an agent that weakens the ligament. This process would facilitate TCL elongation by the inducement of tissue degradation. One possible solution might lie in enzymatic degradation which has already shown to effectively influence the mechanical properties of several tissues.^(6,8)

2.0 SPECIFIC AIMS

2.1 AIM 1

A ligament's function is dictated by its collagen network in view of the fact that types I and III collagen are the main load bearing constituents within the extracellular matrix for most types of ligaments. ⁽⁴²⁾ Such fibers could be inserted on several bones and determine the material response of a ligament. However, some ligaments, especially within the knee, only have two insertion sites which infer a highly anisotropic response because their insertion anatomy is simplified. Similar to other ligaments, the TCL's main constituents, other than fibroblasts, consist of type I and III collagen with a small portion of elastic fibers. ⁽¹⁸⁾ However, in contrast to most knee ligaments, it inserts on multiple bones as previously stated and infers a complex material response in addition to its complex function (Chapter 1). Thus, a ligament's fiber orientation, along with its respective mechanics, proves to be important in the determination of a ligament's physiology.

Little research has been done concerning fiber orientation of the TCL; in fact, the majority of research has been observational. This general observation of alignment is used by surgeons to locate the TCL and to distinguish it among other nearby tissues. ^(16, 18) This general observation of alignment is used by surgeons to locate the TCL. ⁽¹⁶⁾ A contrasting study disclosed that there are not only transverse bundles of fibers that exist within the TCL but also additional oblique fiber bundles in which the ligament's depth dictates the type of fiber bundle. ⁽³⁾ Therefore, further research needs to be done to determine the load bearing directions of the TCL; whereas, fiber orientation, throughout its depth, has yet to be quantified statistically. Our objective is to determine these preferred directions within the TCL with the small angle light scattering technique (SALS). ⁽⁴⁾ We hypothesize that the majority of fibers found within the TCL will be aligned mostly in the transverse direction and will indicate its ability to bear large loads along that axis.

2.2 AIM 2

I have already stated that recent research on the TCL has indicated a significant bearing on the carpal tunnel's compliance; however, its uniaxial properties have yet to be indicated in current and past studies. Initial testing of the TCL within the laboratory has shown that its tangent modulus in the transverse direction was over a factor of ten greater than the tangent modulus in the longitudinal direction. ⁽⁶⁹⁾ Therefore, disparities among load bearing directions indicate the TCL's anisotropic property. Additional tests have been done on carpal tunnel stiffness where compliance tests were performed with an indenter. Moreover, both tests disagree on the TCL stiffness. Li et al found that TCL compliance can reach up to .1 mm/N or up to a stiffness of 10 N/mm; whereas, Holmes et al found much larger values for TCL's stiffness with some values reaching to approximately 42 N/mm. ⁽⁴³⁾ However, such values can't be generalized for TCL stiffness because the mode of testing was indentation, instead of being uniaxial. Similarly, such statements cannot be generalized for the TCL because indentation tests were run while the carpal tunnel contents were left intact. ⁽⁴³⁾ Therefore, the TCL's material properties and its fiber orientation have yet to be accurately quantified.

Collagenase has been used in clinical studies to effectively modify the mechanics of several tissues. Matrix metalloproteinase 1 (MMP1) or collagenase mainly targets or degrades collagen type I which is known as one of the main load-bearing constituents of connective tissues. Colistridal collagenase, which is derived from *Clostridium Histolyticum*, has well-defined proteolytic properties allowing for it to effectively break down the peptide bonds commonly formed within collagen (Fig. 2.1).

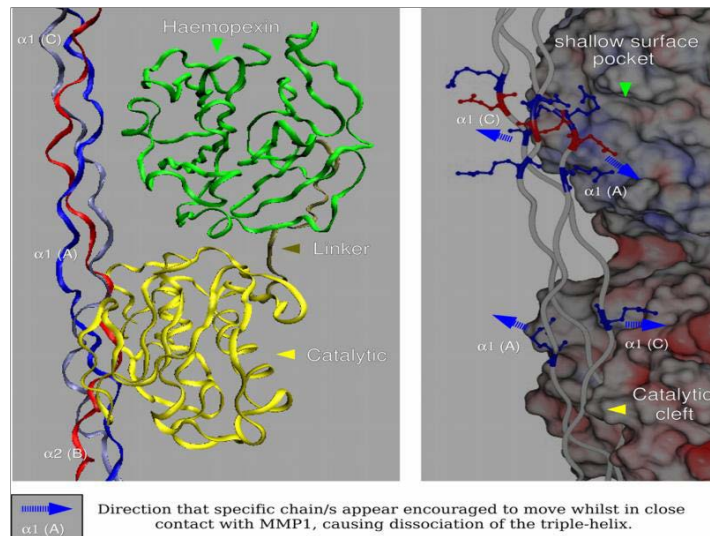


Figure 2.1. (Right) Shows the general structure of collagenase or MMP1 and its interaction with the triple helical structure of type 1 collagen. (Left) Domain organization of MMP1 while in contact with its fibrillar substrate.

It offers advantages over the traditional standard of care of fasciotomy by targeting type 1 and type III collagen. Such enzymes can cleave peptide bonds of collagen and have a specificity for the Pro-X-Gly-Pro-Y region, splitting between X and Gly.⁽⁴⁴⁾ However, such enzymatic degradation does subject the patient to tendon and neurovascular injury due to nonspecific enzymatic degradation.⁽⁴⁵⁾ Previous completed research implemented colistridal collagenase by injecting it in rabbit tails where substantial collagen lysis in the tendon was found.⁽⁴⁵⁾ In past studies, colistridal collagenase has been shown to have considerable merit as a non-surgical treatment for other hand complications.^(6, 46, 47) However, minor adverse reactions, including site tenderness, mild hand swelling, minimal hematoma, or forearm tenderness, do occur with these symptoms.⁽⁴⁶⁾ Inappropriate collagenase injection will result in subsequent damage to various tissues. Thus, careful insertion of the needle has to be considered when it is administered to patients. However, such features have not prevented its use in the clinical setting.⁽⁴⁸⁾

Tissue pathologies, which were successively treated with collagenase, consist of pathogenic chords, leg ulcers, plaques, scar tissue, and others. ⁽⁴⁹⁾ Those aforementioned pathologies are generally described as excessive growths of tissue or dysplasia. Therefore, an ideal treatment would have to successively eliminate subsequent abnormal tissue deposition. Although not all pathologies have been addressed, Dupuytren's contracture (DC), which causes pathogenic chords to form within the hand's palmar fascia, has been shown to be treated effectively with collagenase. ^(6, 46, 47) Basic protocol for treating the chords consists of injecting collagenase followed by force application to break the tissue causing contracture; whereas, collagenase degrades the mechanical properties of the pathological tissue. ⁽⁴⁶⁾ Recent studies on collagenase have shown its efficacy to change the mechanical properties of several tissues.

The addition of collagenase has been shown to effectively change the mechanics of various types of connective tissue, muscle tissue, and epithelial tissue. Significant changes can be seen within ligament's mechanical properties as well as its viscoelastic properties. Usual changes consisted of decreases in its loading capacity with subsequent changes to the tissue's stiffness, tangent modulus, and ultimate stress; such were contrary to its extensibility in which associated increases were found. Thus, modified tissue function would ensue from those aforementioned subsequent changes. Therefore, since an enzyme can be used to alter a respective tissue's function, our objective is to determine whether it could be used to preferentially degrade the TCL's mechanical and structural properties. Such findings could corroborate using collagenase as an alternative therapy for CTS.

3.0 FIBER ORIENTATION OF THE TCL

3.1 OBSERVATIONS OF TCL FIBER ORIENTATION

Current work on the TCL has been scarce and limited. Morphology of the TCL has been studied in the past to understand its structure in terms of thickness and proximal-distal length. General and experimental observations have also shown the TCL to have a dense and inextensible collagenous matrix with a predominant alignment in the transverse direction. Other studies have determined the various fiber configurations of the TCL.

Isogai completed an extensive study on the general fiber alignment within different laminae of the TCL. Two configurations were shown to be the most prominent with both of the arrangements having transverse and oblique fiber variations for its volar and its deep layers. Type 1 configuration reveals a distal transverse bundle of fibers as well as a proximal ulnar-oblique bundle of fibers throughout the TCL's thickness (Fig. 3.1).⁽³⁾ The second configuration of the TCL was observed to have a type 1 configuration for its superficial layer; however, its deep layer consists of a distal radial-oblique bundle along with a proximal transverse bundle (Fig. 3.1).⁽³⁾

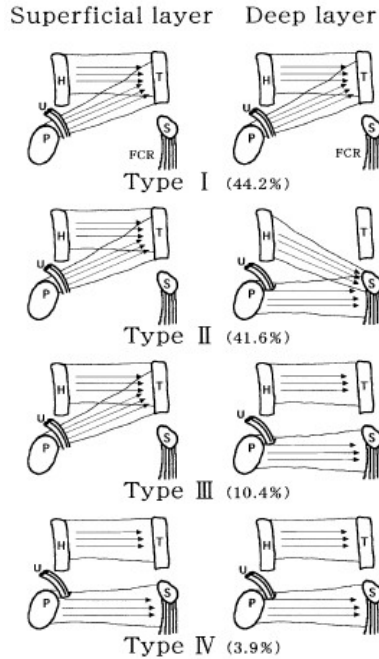


Figure 3.1. Shows the laminar configurations observed for the TCL.⁽³⁾

Other configurations were shown to be marginal within the large, sample size. Both the third and fourth configurations have mainly transverse bundles with the third configuration displaying a superficial, proximal bundle of ulnar-oblique fibers for its distinguishing characteristic (Fig. 3.1).⁽³⁾ Overall, current knowledge of the fiber orientation of the TCL is rather rudimentary; whereas, the studies were observational in analyzing fiber orientation.

3.2 SMALL ANGLE LIGHT SCATTERING

The small angle light scattering (SALS) technique was developed to map the preferential directions of the fiber structure within soft tissues.⁽⁴⁾ Figure 3.2 depicts the general flow of information and its imaging premise for collagen fiber orientation.

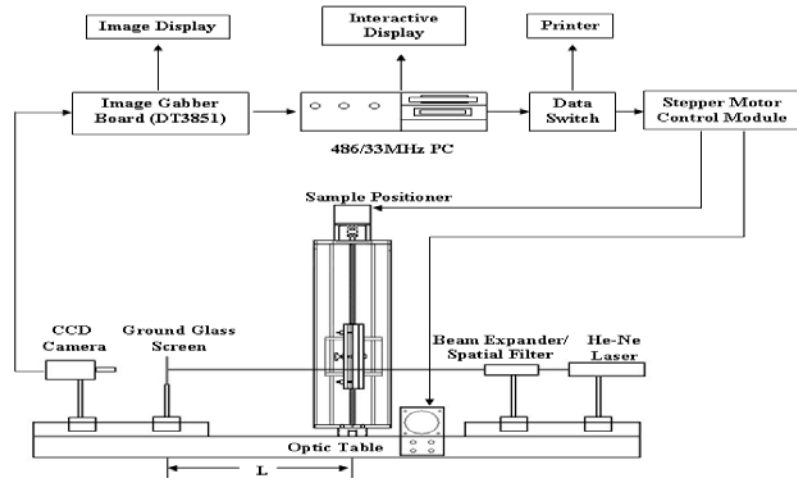


Figure 3.2. Experimental setup for SALS (adapted from Sacks et al.).⁽⁴⁾

Previous validations of this methodology have shown that this technique can measure fiber orientation for up to at least 500 μm along with an angular resolution of $\sim 1^\circ$. Spatial resolution can reach up to $\pm 254 \mu\text{m}$; in this area, preferential fiber direction can be determined. Past studies quantified the fiber orientation of heart valves⁽⁵⁰⁾, cornea⁽⁵¹⁾, cranial dura mater⁽⁵²⁾, glenohumeral ligament⁽⁵³⁾, and remodelling of collagen fiber alignment⁽⁵⁴⁾. However, no study incorporates its usage to determine quantitatively preferred fiber directions of the TCL.

The purpose of this study was to use this SALS technique to characterize the orientation of the TCL's collagen fibers. I hypothesize that the overall majority of fibers would be transverse with some fibers orienting obliquely inserted either from the pisiform bone onto the trapezium or from the scaphoid onto the hamate.

3.3 TCL FIBER QUANTIFICATION

3.3.1 Experimental preparation

The process used to analyze the TCL was broken down into five phases: dissection, fixation, tissue sectioning, image preparation, and SALS imaging. The process took approximately four days to complete. Data processing and statistical analyses were additionally completed to reveal preferential fiber orientation throughout the depth of each TCL.

The dissection and fixation stages took place on the first day. This process allowed for the removal of TCL to be preserved before slicing and imaging. Eight fresh frozen hand specimens (53 ± 13 years) were selected through review of their medical history record to exclude those found with muscular-skeletal injuries or surgeries to the hand and the wrist. The dissection was directed to remove the skin and soft tissue attached to the volar side of TCL. The TCL was identified as a dense, thick, and fibrous bundle of collagen. Further isolation was carried out through identifying its insertion sites on the carpal bones. The tissue insertions were removed, and the ligament was subsequently cleaned.

Fixation of the tissue was performed immediately after its removal with its immersion in 10% phosphate buffered formalin for 24 hours. Then, the tissue was frozen in -20°C temperature for another 24 hours. The embedding and slicing stages took place on the third day. Specimen thickness was measured with digital calipers while the tissue was still frozen. Two holes were punched out through the thicknesses at the mid-points of the proximal and distal ends to define a midline along the proximal-distal direction of the TCL. Each ligament was mounted in a medium set at optimum cutting temperature and placed within a cryostat (Microm®, Thermo-Scientific; Waltham, MA), which preserved the tissue at a temperature of -20°C . The cryostat was set to slice the specimen at $20\ \mu\text{m}$ thickness increments. Sections of interest were obtained on glassmicroscope slides at 25% (volar), 50% (middle), and 75% (dorsal) of the TCL thickness or its depth with 0% signifying its volar side. All slides were kept within a specimen freezer

set at -20°C until imaging. Each slide was placed in glutaraldehyde solution for 5 minutes. This solution increased the slide's transparency by dissolving any extraneous artifacts left on the slide. Slides were rinsed in distilled water and then left to dry. All slides were cleaned with individual wipes and glass cleaner.

Each slide was placed in the sample holder of the SALS apparatus to be individually scanned. The processing stage consisted of the imaging phase which consisted of several steps. SALS imaging has been utilized in previous works and its approach has been well established. ⁽⁴⁾ Briefly, an unpolarized 4 mW HeNe laser was directed on to the slide. The positioning of the light beam was centered on the camera's lens scan for the total area of the tissue section. This was accomplished with the movement of the spatial filter-beam expander and the camera. Scattered light data was gathered and digitized by using an image grabber board in conjunction with the camera to obtain the fiber network orientations across each tissue section.

3.3.2 Imaging preparation

Orientation data was accumulated for each scanned area in the form of light intensity distributed over angles covering one revolution. This area was equivalent to a circle with the diameter of 254 μm . ⁽⁴⁾ Each intensity distribution withholds two concerning variables: the preferred fiber direction and the orientation index (OI). ⁽⁴⁾ The analysis of each slide led to an image which displayed these features for each scanned area spanning the entire tissue section.

The distribution centroid represented the overall preferred direction for the fibrous network located within each scanned area. ⁽⁴⁾ Accuracy of the estimated preferred direction could be inferred from the difference between each light intensity distribution's centroid and its corresponding angle of peak intensity. ⁽⁴⁾ A large difference indicated that a large skew was present. Possible reasoning behind this significant skew could be that many different fiber networks, which were aligned in multiple directions, overlaid each other within the designated scanned area of the tissue section. In the case where a small skew was present, fiber networks

were coincident in the measured preferred direction and validated the centroid measurement. A simple verification for the preferred direction can incorporate the OI which determines the angle at which one-half of the total fibers are oriented. This is determined through the difference between the maximum and minimum angle of the range where one half of the total area of the light intensity distribution is situated. ⁽⁴⁾ Highly oriented, scanned areas have low OI values while randomly oriented; fiber networks have large OI values. ^(4, 54)

Several adjustments had to be made, in order to analyze the fiber orientations within each depth. The preferred directions had to be corrected to the proximal-distal midline of the TCL, and artifacts had to be removed. The former was completed based on the inspection of the two holes within each tissue section's resulting SALS image. Original preferred directions were subtracted by this value. The latter efforts entailed removing cutting artifacts by utilizing an OI value of 45 to isolate actual fiber orientations and to disregard areas with multiple fiber directions. ⁽⁵³⁾

3.3.3 Data processing

Histograms of the preferred directions for each depth were created to see if a pattern of fiber orientation existed. The frequency of preferred directions for each angle spanning 0°-180° was normalized with respect to the number of scanning areas within each tissue section. Normalized frequencies of all sections for each depth were added across different specimen and averaged. Four types of fiber orientations for each section were considered: Transverse (0°-22.5°, 157.5°-180°), Oblique in the pisiform-trapezium direction (PT Oblique, 22.5°-67.5°), Oblique in the scaphoid-hamate direction (SH Oblique, 112.5°-157.5°), and Longitudinal (67.5°-112.5°). See Figure 3.3. Percentages of the preferred directions for the four orientations were calculated within those ranges.

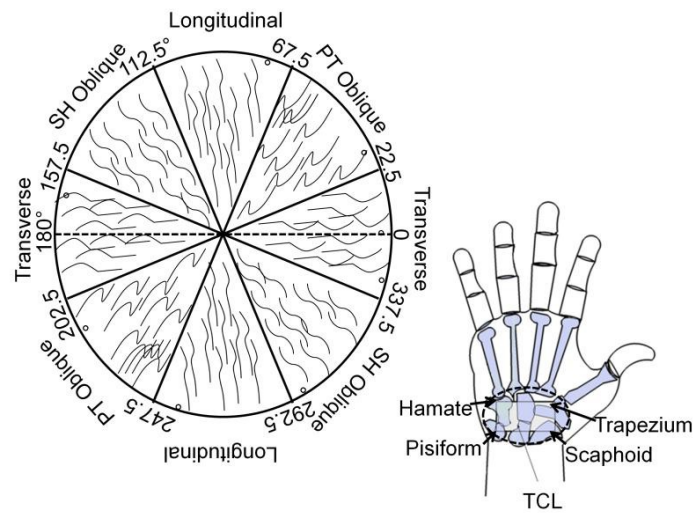


Figure 3.3. Shows the designated fiber ranges of interest where a circle was divided into the above, four regions: transverse, scaphoid-hamate (SH) oblique, pisiform-trapezium (PT) oblique, and longitudinal.

The Watson-William's test investigated the differences of fiber alignment with respect to thickness depth. ⁽⁵⁴⁾ Fiber alignment was quantified by using the angular dispersion of preferred directions for each section. ⁽⁵⁴⁾ This measurement is equivalent to calculating the standard deviation of an array of data tabulated on a circular scale. Overall, the analysis attempted to compare the spread of preferred directions of fiber networks among different depths. Groups were compared for superficial, middle, and deep sections with the significance set at 0.05. A subsequent one-way analysis of variance (ANOVA) calculated the differences among the types of different fibers if differences across depths were non-significant. In the case of a difference, a two-factor mixed measures ANOVA was employed. Additionally, prerequisite assumptions were also checked; and if any inconsistencies were found, the equivalent non-parametric test was employed. Pairwise comparisons determined whether differences existed between each group. Differences were considered at $\alpha=0.05$ for all statistical analyses.

3.4 RESULTS

3.4.1 Laminar changes within fiber orientation

Sample SALS outputs revealing the variables of the preferred directions and the OI are shown in figure 3.4. The green specks signify the angles of orientation for each scanned area, i.e. preferred directions. The underlying colored areas for each scanned area represented the order of alignment or the OI. Red and purple areas signify highly aligned fiber networks while green and blue areas signify sparsely arrayed fiber networks directed over the area (Fig. 3.4). The SALS outputs for 25%, 50%, and 75% depths display visible differences for the degree of alignment where fibers appeared more sparsely arrayed for the 25% depth in comparison to the specimen's deeper depths (50% and 75%, Fig. 3.4).

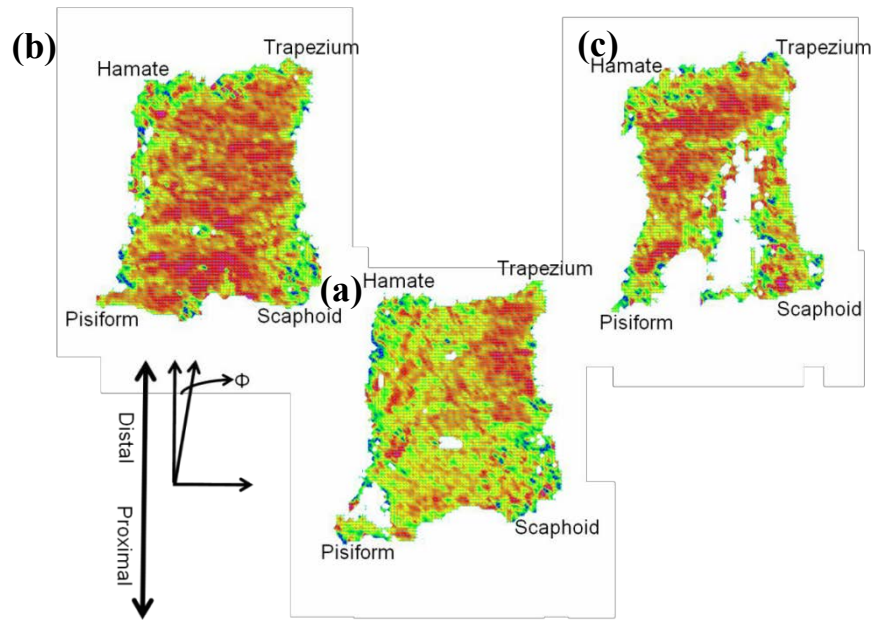


Figure 3.4. SALS outputs for the various depths of a respective specimen (a) 25% depth, (b) 50% depth, and (c) 75% depth (0%: volar side of TCL).

Fiber alignment for the section depth was determined by the use of circular statistics. A trend was indicated by visibly inspecting each circular histogram at different layers of the TCL (Fig. 3.5).

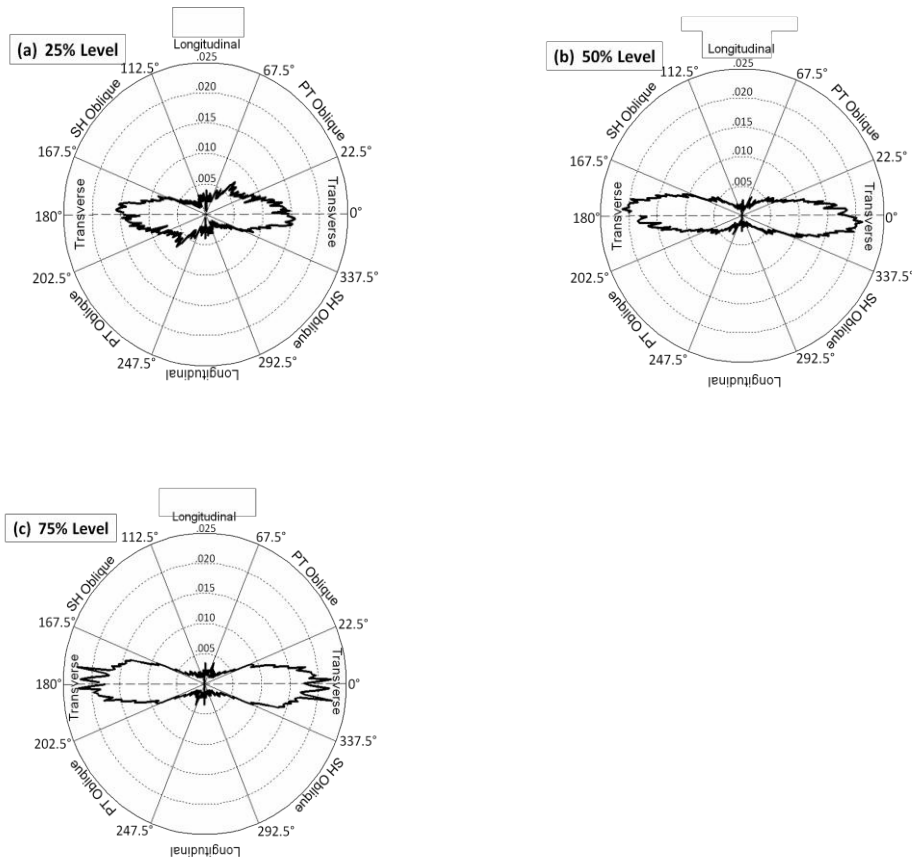


Figure 3.5. Average histograms of preferred fiber directions at (a) 25%, (b) 50%, and (c) 75% depths (0°: volar side of TCL).

However, the Watson-Williams test showed results with this trend as insignificant where fiber orientation did not vary with respect to tissue level ($P > 0.25$). Overall, the tissue section of 50% depth reveals the representative pattern of fiber orientation throughout the depth of the TCL (Fig. 3.5b).

3.4.2 Fiber percentages

Fiber percentages were additionally found to be non-normal; therefore, the appropriate non-parametric test was found to be a Friedman's ANOVA. The aforementioned test compared among different types of fiber orientations and neglected the thickness depth. Overall, the test

found a large significant difference among the different types of fiber orientations ($P < 0.0001$). Post-hoc testing for fiber percentages indicated that the transverse fibers were the predominant type of fiber; they were followed by oblique fibers and longitudinal fibers (Fig. 3.5 and 3.6). Overall averages included the following: $60.7 \pm 13.7\%$ for the transverse fibers, $18.6 \pm 10.6\%$ for the PT Oblique fibers, $13.0 \pm 6.7\%$ for the SH Oblique fibers, and $8.6 \pm 5.1\%$ for the longitudinal fibers.

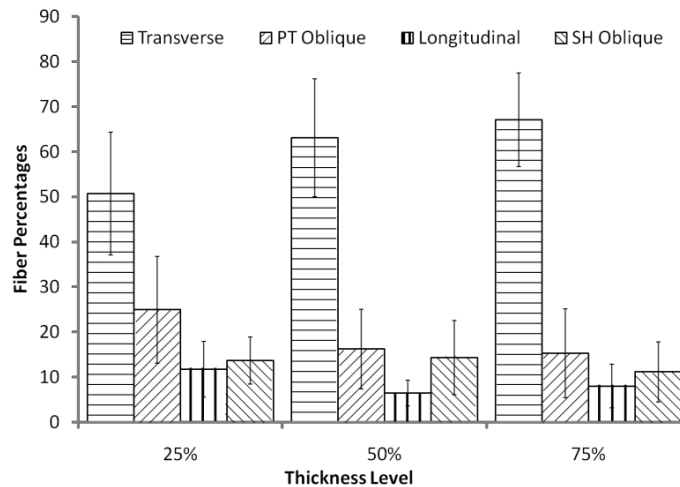


Figure 3.6. Fiber percentages measured with respect to slice depth (0%: volar side of TCL).

3.5 DISCUSSION

3.5.1 The collagen fiber orientation of the TCL

The TCL was found to have a preferred degree of fiber alignment which suggested material anisotropy. The results showed that the predominant fiber direction was transverse while longitudinal and oblique fibers were marginal. These findings were validated by our laboratory; initial testing of the TCL showed that the tangent modulus was many times greater in the transverse direction than that in the longitudinal direction which was demonstrated by Xin et al.

⁽⁶⁹⁾ This anisotropic property should be considered for future modeling applications.

Results revealed that the fiber distribution did not change with respect to depth, but significant differences were found in comparison across the different types of fiber orientations. Our data are consistent with the gross observation⁽³⁾ and staining methods⁽¹⁸⁾ in that TCL fibers were predominately aligned in the transverse direction. In an observational study, Isogai et al. (2002) reported that the fiber laminar configuration varied from specimen to specimen and categorized them into four types of fiber orientation. Type I configuration is distal transverse and ulnar (pisiform to trapezium) oblique in every laminae of the TCL; type II configuration is distal transverse and ulnar (pisiform to trapezium) oblique in the superficial layer with proximal transverse and radial oblique (scaphoid to hamate) in the deep layer; type III configuration is distal transverse and ulnar oblique in the superficial layer and proximal/distal transverse in the deep layer, and type IV configuration is transverse at all depths with no clear oblique fibers. However, our data demonstrated that the orientation pattern did not differ among the volar, middle and dorsal layers. Therefore, the bilaminar configuration of the TCL doesn't appear within our results.⁽³⁾ Thus, the incidence of incomplete release might not be due to the prominence of a superficial and distal transverse bundle. Though our study provided more quantitative results of TCL fiber orientation, future studies using a larger sample size may help to confirm the types of laminar configuration observed by Isogai et al. (2002). However, such an increase in sample size might be futile; whereas, statistical significance was found to be very small ($P < 0.0001$) which indicated large differences.

Predominance of the transverse fiber orientation could play an important role in maintaining the carpal arch. This inference made us believe that a significant portion of transverse stability is provided by the TCL; whereas carpal arch expansion in the oblique or longitudinal directions may not be as important. Such directionality was also featured in measuring changes to carpal tunnel compliance before and after TCL transection.^(25, 27) In an unloaded state, the TCL fibers may display a wave form configuration.⁽¹⁸⁾ This means that the same fiber may have different

orientations at different points along its length. The orientation indices based on regional information may not accurately correlate with the amount of fibers in a certain direction. A possible improvement could be to load the TCL sample during tissue fixation. ⁽⁵⁵⁾

3.5.2 Future model implementation

Fiber orientation has a significant effect on the accurate representation of a tissue's mechanical properties. ⁽¹⁴⁾ Sacks et al have shown that SALS data may be incorporated within a finite element model and, thus, improve the accuracy of the model. ⁽¹⁴⁾ Thus, similar exploits could be utilized within a finite element model representing the carpal tunnel.

SALS has been shown to accurately determine the angular distribution of most fibrous networks for various tissues. Lanir et al. could have proposed the most complete approach for structural modelling for soft tissues; whereas, such theory has been implemented in an effort to accurately represent several tissues. ^(14, 56) Its structural implementation is dependent on the angular distribution of collagen, $R(\theta)$ and can be determined from the mean scattered light distribution ($I(\theta)$) measured from an imaging modality using small angle light scattering (Eqn. 3.1). ^(14, 56)

$$(3.1) \quad R(\theta) = \frac{\bar{I}(\theta)}{\sum_{\theta=-\pi/2}^{\theta=\pi/2} I(\theta)\Delta\theta}$$

However, such measurements were not only made with the concerning tissue while in its reference state but also while subjected to several biaxial strains; whereas our experiment only measured fiber orientation within its reference state. Thus, future studies might look into multi-loading the TCL specimen, in addition to measuring such states' corresponding fiber orientations.

4.0 INITIAL OBSERVATIONS OF COLLAGENOLYTIC EFFECTS

4.1 THE BIOLOGY OF COLLAGENASE DEGRADATION

The principle of collagenase dissociation is simple; the extracellular matrix proteins of the tissue are subjected to matrix metalloproteases which are selectively digested based on environmental factors. Several routine applications enforce enzyme dissociation for tumors or islet cell isolation where such enzymes are derived from either bacterial source or animal source. ⁽⁵⁷⁾ Unfortunately, no generic approach is available to dissociate the various types of tissues digested.

The extra-cellular matrix (ECM) of a tissue determines its physiology and is made up of four main components: collagen, elastin, glycoproteins and proteoglycans. ⁽⁵⁷⁾ Each of these components can be further divided into different subtypes and concentration, which vary for different tissues. In particular, a tissue's collagen content is determined to be one of the main constituents of the ECM that contribute significantly towards its mechanical properties; therefore, enzymatic degradation, that is incurred by collagenase, may have a significant effect on a tissue's mechanical properties.

To simplify the complexity of collagenase's enzymatic process, I have focused on enzymatic degradation of collagen through the use of *Clostridium histolyticum* collagenase; this enzyme is produced in commercial scale from pathogenic bacteria like *Clostridium histolyticum* which employs it for invading the host organism. Bacteria - derived collagenase behaves similarly to tissue collagenase; however, bacteria - derived collagenase attacks multiple sites of tropocollagen while tissue collagenase targets only one site. Modeling studies have emphasized the interaction between collagen and collagenase. Such interaction demonstrates that the enzyme

tends to mimic its collagen substrate's conformation. This conformational change allows for the enzyme to disturb collagen's quaternary organization of the triple helix, specifically the proline portion of collagen. Furthermore, the proline hinge domain of collagenase forms a "proline-zipper" with two helices of collagen's triple helix which proves to be a key step in destabilizing collagen. Collagenase's active site consists of two histidine residues which act as binding ligands for the zinc ion.⁽⁵⁸⁾ Catalytic activity incurs when the zinc ion, located within the enzyme's central core, promotes an attack on the electron distribution within collagen by targeting the carbonyl carbon by an oxygen atom of a water molecule at the active site.⁽⁵⁸⁾ Within the active site, a base facilitates the aforementioned reaction by extracting a proton from the associated water molecule.

Varying mixtures or crude measures of collagenase, which include non-specific proteinases along with elastase, have been created. Bacterial collagenase can be separated into two classes: class I collagenase (α , β , γ) and class II collagenase (δ , ϵ , ζ); whereas, tissue collagenases have shown to be more specific in their activity.^(57, 59, 70) Similarly, more purified collagenases can also be created. Table 3.1, which was originally developed from Bhavya's thesis, shows several measures of specific activity for different types of collagenase which were original experiments conducted by Bond et al.^(57, 59, 70) Within the table, specific activity for different types of collagenase was measured by using ($^{14}\text{CH}_3$)-collagen and synthetic polypeptide 2-furanacryloyl-L-leucylglycyl-L-prolyl-L-alanine (FALGPA).^(57, 59) Specific activities for additional proteinases were quantitatively measured by using N- α -benzoyl-L-arginine ethylester (BAEE) and ($^{14}\text{CH}_3$)-casein.^(57, 59)

Table 4.1. the measured activity of various types of collagenases from commercial source (Bond MD 1984, Source: Bhavya 2006) ⁽⁷⁰⁾: ^aThe mass of crude powder was determined by weighing the preparation, as received, while the milligrams of protein were determined by the dye binding assay. ^bsp. Act. is less than 0.0010 nkat/mg. ⁽⁷⁰⁾

Supplier	Designation	Lot #	mg of protein/ mg powder	Specific activity (nkat/mg of protein)			
				[¹⁴ CH ₃]-collagen	FALGPA	BAEE	[¹⁴ CH ₃]-casein
		Crude preparation					
Sigma Chemical Co.	Type I	121F-516	0.37	0.0029	2.8	540	1.9
	Type IA	101F-6831	0.46	0.0013	1.0	25	0.27
	Type II	91F-6812	0.26	0.00045	0.30	58	0.13
	Type IV	42F-6838	0.43	0.0023	3.0	77	0.71
	Type V	11F-6805	0.43	0.0033	2.7	160	0.54
	Z-9999	81F-6819	0.37	0.0038	4.8	98	0.80
Worthington Biochemical Co.	Type I	42C008	0.46	0.0022	2.6	250	1.9
	Type II	W2H209	0.33	0.0023	3.2	650	2.0
	Type III	41S130	0.36	0.0023	2.7	36	0.80
	Type IV	41S123	0.74	0.0024	2.4	490	0.27
Roche-Manheim	None	11451142	0.39	0.0023	2.3	440	1.1
Advanced Biofractures Corp.	ABC-TD	111-051082	0.23	0.0020	4.9	43	0.17
	ABC-I	P-78R	0.20	0.00060	0.65	100	0.13
	ABC-II	P-79-02R	0.17	0.0010	0.76	120	0.18
	234,222	103310	0.12	0.00065	1.2	130	0.16
	23,415	102346	0.20	0.0013	2.9	44	0.19
Partially purified preparation							
Sigma Chemical Co.	Type III	61D-0566	0.90	0.0077	7.8	720	0.087
	Type VII	111F-6831	0.77	0.0017	78	5.5	0.0011
Worthington Biochemical Co.	CLOSA	51H319	0.49	0.00065	38	1.3	0.030
	CLSPA	W2J452	0.72	0.012	11	72	b
Advanced Biofractures Co.	ABC-III	186E	0.11	0.020	19	3.0	b
Calbiochem	234,136	130075	0.15	0.0092	8.0	250	0.0075

4.2 OBSERVATION PROCEDURE

An ideal concentration was determined by the observational effects of several intercarpal ligaments. Several concentrations, based on collagenase digested units (CDU) or units (U), were used, and the effects of five different concentrations of collagenase were studied.

Crude collagenase's activity is dependent upon several environmental factors such as calcium concentration; therefore, its incorporation within phosphate buffered saline (PBS) was necessary to digest any tissue. Sigma-Aldrich phosphate buffered saline (PBS) fortified with calcium chloride was utilized to activate the enzyme. Similarly, Sigma-Aldrich type I collagenase was also used with a conversion ratio of 278 CDU/mg, and the following concentrations were created: 300, 500, 700, 1000 and 1200 units. Associated masses were measured with a scale that weighed accurately to a microgram. Each ligament was submerged within a mixture of a designated amount of collagenase and a roughly measured amount of two milliliters of the aforementioned buffer.

In obtaining ligaments for observation, one cadaveric hand was used. Careful removal of the dorsal skin flap and musculature was exercised before any removal of the ligaments. Figure 4.1 displays a portion of intercarpal ligaments that were isolated for this observational study. Removed ligaments included the following: the dorsal intercarpal ligament, the extensor retinaculum, and the dorsal radiocarpal ligament. The extensor retinaculum wasn't shown because it was the most superficial ligament out of three; it formed a soft tissue extension similar to its counterpart, the flexor retinaculum. Since there were more than three concentrations, some ligaments had to be divided into multiple strips (for example, the dorsal radiocarpal ligament and the extensor retinaculum.) Designated mixtures were as follows: 300 U – extensor retinaculum, 500 U – dorsal radiocarpal ligament, 700 U – extensor retinaculum, 1000 U – dorsal intercarpal

ligament, and 1200 U – dorsal radiocarpal ligament. Initial and hourly observations consisted of looking at the tissue to see if any noticeable differences progressed as well as manually applying tensile forces with forceps to see if collagenase weakened the tissue. Pictures and observations were taken before collagenase application and, thereafter, after each hour up to a total of four hours of treatment.

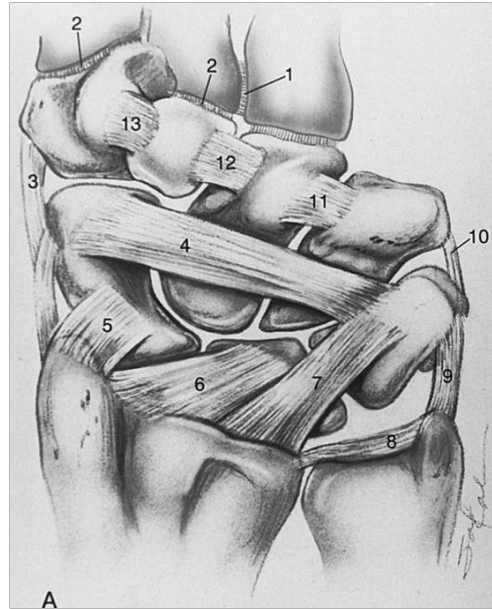


Figure 4.1. Displays the ligaments that were used for the initial observations of collagenolytic effects; whereas, (4) is designated for the dorsal intercarpal ligament while (5) is designated for a portion of the dorsal carpal ligament which is located just superficial to the dorsal intercarpal ligament, respectively (Source: Goldfarb et al. 2001).

4.3 RESULTS

Photographed specimens are shown in figure 4.2 where the hourly observations are shown in the preceding, table 4.2. Both the figure and the table are divided with the hours and the concentrations shown at the top and the left for the respective figure and at the left and the top for the respective table.

Table 4.2. Shows the written observation of subsequent changes to respective ligaments with the addition of several concentrations of collagenase. Observations were made at each hour up to a total four hour for treatment duration.

Ryan Prantil		Collagenase Effects on Various Dorsal Wrist Ligaments			
9/2/2010					
Ligaments Used	Extensor Retinaculum Piece 1	Dorsal Radiocarpal Ligament Piece 2	Extensor Retinaculum Piece 2	Dorsal Intercarpal Ligament	Dorsal Radiocarpal Ligament Piece 1
Concentrations(units)	300	500	700	1000	1200
Times(hr)					
1	No Difference	No Difference	No Difference	No Difference	Difference- Some Degradation
2	No Difference	No observable differences. But did rip with applied tensile forces.	Little Difference. Appears very stiff with no give with applied tensile forces.	Fibers appear spread apart and found to be weaker with applied force.	Fibers were found to be spread apart. Was found to be weaker with applied tensile forces.
3	No Difference	No Difference	Fibers appear to be peeling and are spread apart.	Could be pulled apart easily. Fibers are spread apart.	Fibers again appear spread apart.
4	Fibers starting to peel and there appears to be a little slack.	No huge difference, but some changes have occurred.	Fibers are starting to separate and there is a decrease in strength.	Tissue is close to being degraded completely. With applied forces, fibers appear to be ripping.	Tissue appears degraded and ripped apart with little applied tension.

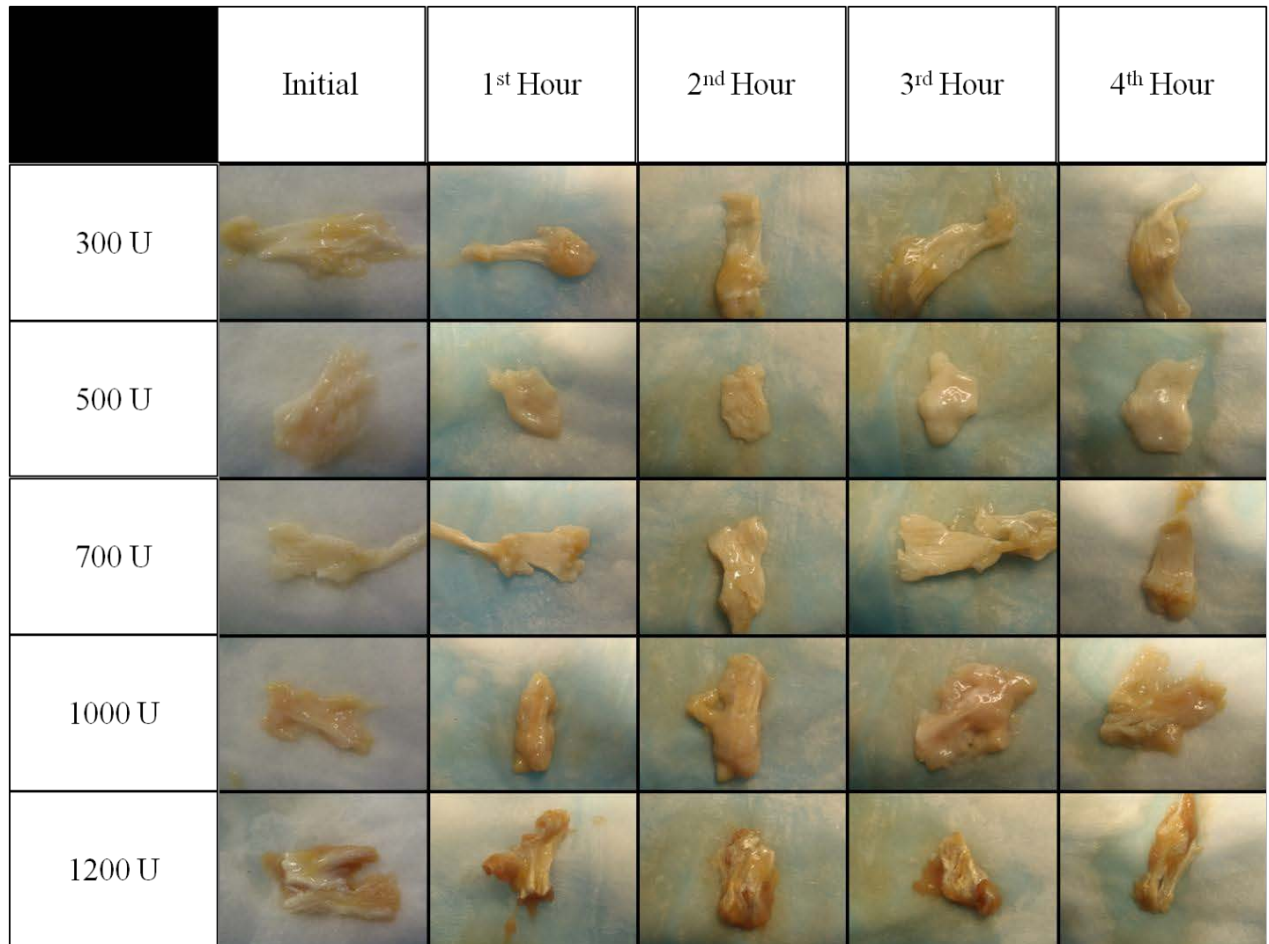


Figure 4.2. Showed the subsequent effects that collagenase had on the aforementioned dorsal wrist ligaments.

4.4 DISCUSSION

The first two concentrations of 300 and 500 units appeared to have small effects on portions of the extensor retinaculum and the dorsal radiocarpal ligament. In contrast, 700 units of collagenase showed apparent changes within the other portion of the extensor retinaculum after three hours of treatment. Furthermore, observable differences stemmed from changes within the microstructure where visual changes in fibers appeared to peel and to separate; thus, this process proceeded to cause a considerable decrease in strength within the extensor retinaculum after the fourth hour of treatment. Fiber degradation advanced more quickly with the application of larger concentrations of collagenase, or more

specifically 1000 and 1200 units; whereas, after the second hour of treatment, noticeable physical changes were apparent along with the aforementioned changes within microstructure.

Based observation, control of temperature, and proper molarity of Calcium proved not to affect the activity of collagenase drastically. Significant degradation of the ligaments' microstructure was found for all dorsal wrist ligaments, especially for concentrations higher than 700 U of collagenase. The structure of type I collagen is made up of two alpha I subunits and one alpha II subunit. ⁽²⁾ Similarly, type III collagen also forms a triple helix of three alpha I subunits; however, these subunits have a different structure in comparison to alpha I subunits found in type I collagen. Additionally, the ligament microstructure mainly contains type I and III collagen; however, since bacterial collagenase is not as specific as tissue collagenase, it can be employed to degrade preferentially the structural collagen within ligaments such as the TCL.

5.0 COLLAGENASE'S EFFECTS ON TCL MECHANICS: PRELIMINARY STUDIES

5.1 THE EFFECT OF COLLAGENASE ON TISSUE MECHANICS

5.1.1 Effects on elasticity

Collagenase application can effectively degrade the elastic mechanical properties of a soft tissue because it specifically targets its collagen. The tensile properties of several tissues have been shown to be degraded by collagenase: DC pathogenic chords, rat periodontal ligaments, rat diaphragm muscle strips, guinea pig lung parenchyma strips, bovine corneal tissues, as well as other tissues. ^(6, 8, 60-63) This treatment complements the treated tissue with not only a decrease in tangent modulus but also with an associated decrease in its ultimate tensile stress along with an increase in ultimate tensile strain. ^(6, 8, 61, 62) Thus, overall drastic changes in a soft tissue's stress-strain curve are incurred after enzymatic degradation targeting collagen.

Previous studies looked at the collagenase effects on the dynamic mechanical properties of tissue damping and elastance. Tissue elasticity can be inferred from elastance; whereas, dynamic testing of lung parenchymal strips from the guinea pig model showed that collagenase digestion didn't have a significant effect on the tissue's elasticity. Moreover, numerous previous studies showed that collagen's influence was necessary with regards to its influence on the tissue's elasticity. ^(61, 64) Rat diaphragm muscle strips and pathogenic chords showed large decreases with their respective stress-strain curves before and after collagenase application. ^(6, 62) Rowe et al determined that rat diaphragm muscle strips treated with multiple concentrations of collagenase showed significant decreases in tensile stiffness; whereas, changes incurred by different collagenase concentrations were found insignificant. ⁽⁶²⁾ In contrast, Starkweather et al.

found that the mechanical properties of DC pathogenic chords are significantly affected when injected with collagenase; their respective stress vs. strain curves of controls versus treated are shown in figure 5.1. ⁽⁶⁾

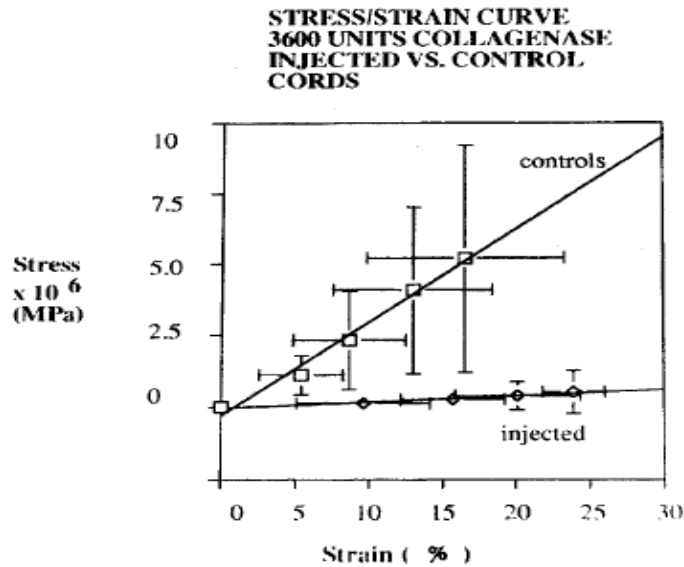


Figure 5.1. Shows the stress vs. strain curves of Starkweather et al. comparing control pathogenic chords to those chords treated with 3600 U of collagenase for 24 hours. ⁽⁶⁾

Although degradation seemed somewhat similar among the two types of tissue, changes proved to be tissue subjective.

Similar to past tissues, research on the collagenase's efficacy on any ligament has also shown drastic changes within its respective elasticity. ⁽⁷⁾ In particular, the majority of research has looked into respective effects on the periodontal ligament as a possible therapeutic agent. Ligament digestion incorporated an enzyme that targeted both type I and III collagen. ⁽⁷⁾ Results showed that enzymatic degradation caused significant changes to the ligament's stress vs. strain curve; whereas, both the tangent modulus and mechanical strength seemed to change significantly. These changes are featured in figure 5.2.

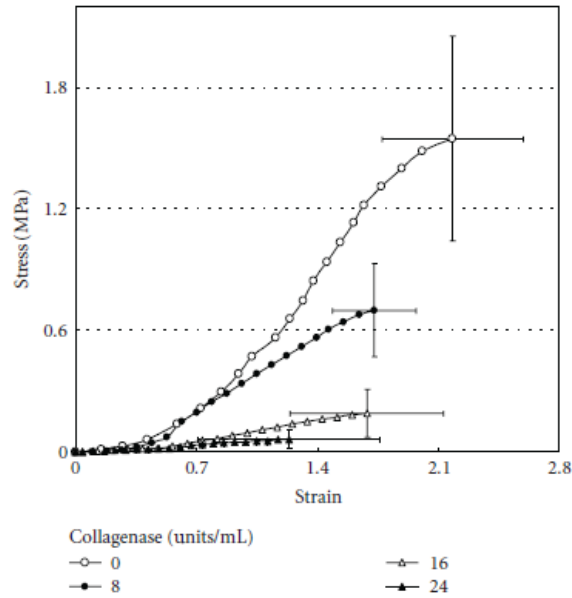


Figure 5.2. Reveals the stress vs. strain curves of Kawada et al. comparing control and various collagenase-treated periodontal ligaments for 4 hours; whereas, the concentrations of collagenase are shown at the bottom. ⁽⁷⁾

Additional research on collagenase effects on the periodontal ligament has been completed concerning its viscoelasticity.

5.1.2 Effects on viscoelasticity

Significant changes can be induced within a tissue's viscoelasticity by using collagenase to digest the respective tissue; whereas, such responses are mechanisms that are chiefly responsible for energy dissipation. Additional definitions of a tissue's viscoelasticity are indicated by the frequency dependence of its complex modulus along with its stress relaxation behavior. Past studies that incorporate collagenase's effect on a tissue's viscoelasticity have explored its compromised response within parenchymal tissue strips from guinea pigs as well as periodontal ligaments from rats. ^(8, 61)

Collagenase-treated and healthy tissues were tested by using dynamic mechanical analyses (DMA) as well as regular stress-relaxation testing. ⁽⁶¹⁾ Yuan et al found that treating rat lung tissue with either elastase or collagenase marginally affected the tissue's hysteresivity while its tissue damping decreases as does its tissue's elastance. ⁽⁶¹⁾ The stress-relaxation response of the periodontal ligament relaxed more rapidly for the collagenase-treated specimens in comparison to the control specimens with those quantitative values approximately being 69.9 and 51.1%, respectively; whereas, each stress-relaxation curve for both the treatment and placebo is shown in figure 5.3. ⁽⁸⁾

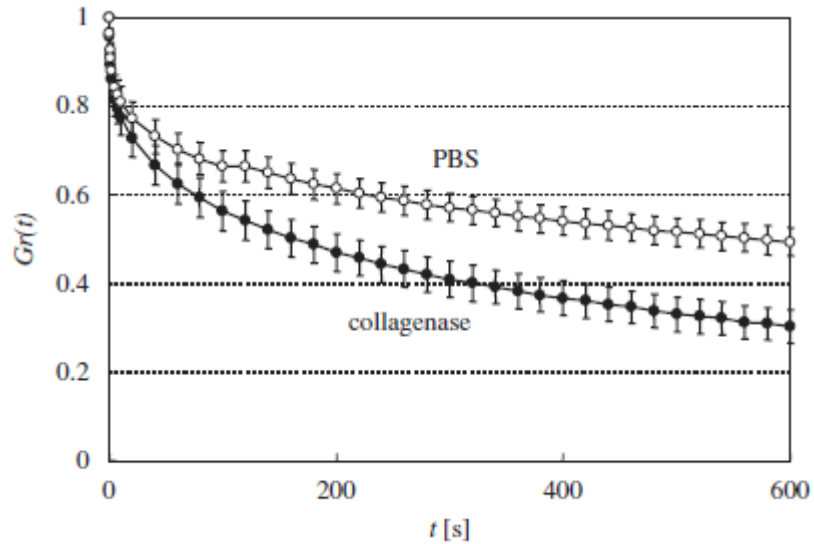


Figure 5.3. Outlines the stress-relaxation curves comparing control and treated periodontal ligaments (Komatsu et al., 2007). ⁽⁸⁾

Furthermore, other differences were found between the treated-group and the control-group with regards to their respective, model parameters. ⁽⁸⁾ Therefore, the periodontal ligament's capacity to relieve stress is increased with the onset of collagen digestion. ⁽⁸⁾

However, instead of determining the collagenase effects on either elasticity or viscoelasticity, we only wish to determine how and to what degree collagenase degrades the mechanical properties of the TCL. Considering past studies on the mechanical properties of tissue and the

application of collagenase, results showed that such properties can be decreased. Thus, I hypothesize that with the use of enzymatic degradation, one can significantly decrease the stiffness of the TCL. With its application, I also hypothesize that collagenase can degrade the TCL's stiffness in linear manner with regards to its time of subjection to collagenase.

5.2 EXPERIMENT 1: STRAINED TO FAILURE

5.2.1 Methodology

5.2.1a Testing protocol

The overall objective of this portion of testing was to determine the mechanical properties of the TCL in the transverse direction while using collagenase to diminish the stiffness of the ligament. Therefore, the steps, in order to achieve the previous statement, consisted of removing several fragments from the TCL and placing each fragment within a certain concentration of collagenase.

This was accomplished through the progression of several stages. Three total specimens were used for testing where the transverse carpal ligament was removed from unknown left and right arms as well as a right hand. At first, one measured the transverse length of each sample with digital calipers. Then, one divided the TCL into five equally-sized tissue strips along the proximal-distal length. Next, each tissue strip was trimmed with a dog-bone shape cutter which had an aspect ratio of 1 to 8. Afterwards, these strips were split up into the five different concentrations of collagenase: control, 500 units, 750 units, 1000 units, and 1250 units. Type 1 collagenase with a conversion of 278 U/mg (Sigma-Aldrich; St. Louis, MO) was implemented within the experimental design. Please note that a scale with an accuracy of a tenth of a microgram was used to weigh out the corresponding mass of each collagenase concentration.

Thereafter, the TCL was placed in a phosphate-buffered saline which was fortified with calcium chloride (Sigma-Aldrich; St. Louis, MO) along with collagenase (depending on its group designation) for three hour duration of time. Please note that all mixtures were kept within test-tubes along with ice surrounding each tube. Each strip was removed from its respective solution after three hours where its thickness was estimated with a linear-variable differential transducer (LDVT) with six estimates taken for each strip. Then, the strip of the TCL was placed on custom-made grips with a snap force of approximately 40 N which is shown in figure 4.4a in the tensile testing apparatus which is shown in figure 4.4b.

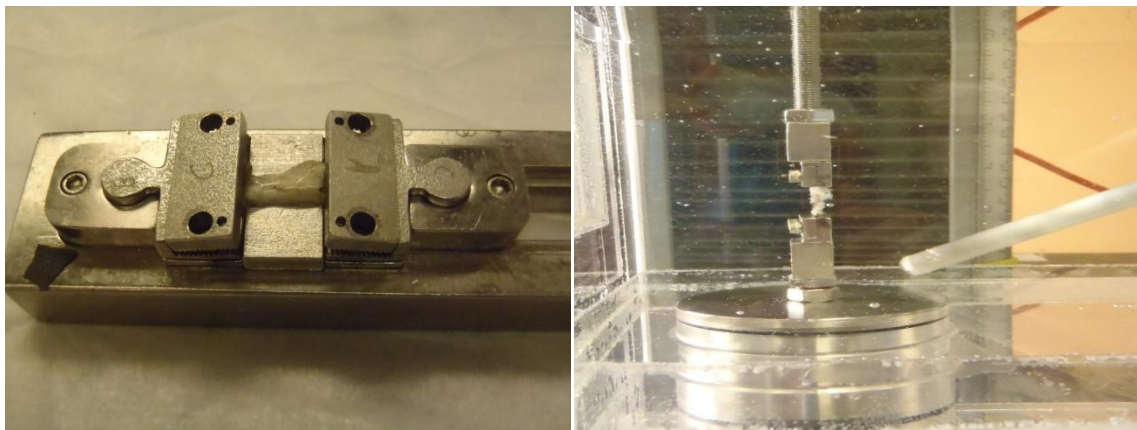


Figure 5.4. Shows how each TCL sample was connected to the testing apparatus (a) its grip placement and (b) its placement within the MTS apparatus.

Each ligament sample was tested while being soaked in heated saline solution. The testing protocol consisted of the following, preconditioning parameters: 5 N for the amplitude, 0.9 N/s for the loading rate, and 10 cycles will be obtained for each test (Figure 5.5). Please note that preceding pilot studies were done to determine such testing parameters.

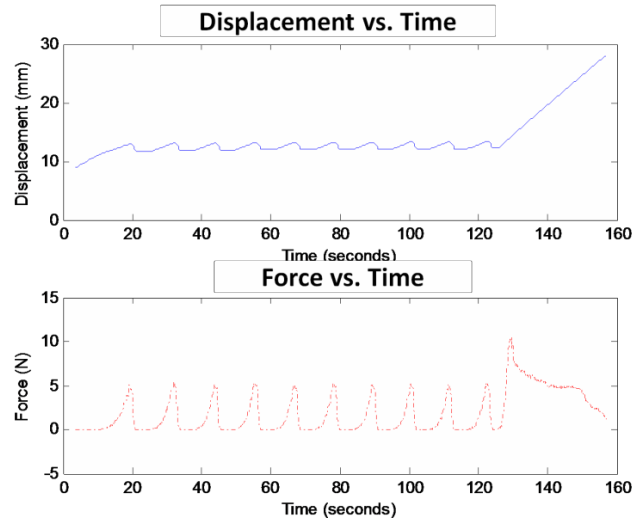


Figure 5.5. Shows the representative testing protocol used for each ligament sample.

Then, the strip was strained until failure. This protocol was repeated for each tissue strip with its different group designation. At the end of each test; the tangent modulus and the ultimate stress were obtained after the strip had been tested until failure. The tangent modulus was calculated using linear regression. Similarly, the strain at failure was also determined. The ultimate stress was determined to be the maximum stress of all stresses while the ultimate strain was only considered at corresponding point of maximum stress. These calculations were determined with the implementation of Excel®.

5.2.1b Data analysis

Mechanical parameters of interest were the following: ultimate stress, tangent modulus, ultimate strain, and stiffness. Stiffness calculation was taken over the region from 1.5 N to 5 N. Such computation was performed by using the situated region's respective points and equation 5.1 to estimate each sample's stiffness; and signifies displacement and force data while and signifies their respective averages. The accuracy of fit for the linear region was

estimated through the use of the coefficient of determination (R^2 , Eq. 5.2), where the sum of squares of the residual or the difference between force data and model estimates are divided by the total sum of squared differences or the difference between the force data and its respective average (Eq. 5.4). Stress and strain transformations were made by using equations 5.3 and 5.4, respectively. Cross-sectional area was calculated as an idealized rectangle where the average thickness measured from the LVDT was multiplied by the sample's width (Eq. 5.5). Strain was computed by using the aforementioned displacement data (Eq. 5.4). Similar proceedings followed the stiffness calculation for the tangent modulus; whereas, equations 5.1 and 5.2 were utilized to compute each sample's tangent modulus with stress and strain substituted with force and displacement parameters.

$$(5.1) k = \frac{\Sigma(d_i - \bar{d})(F_i - \bar{F})}{\Sigma(d_i - \bar{d})^2}; (5.2) R^2 = 1 - \frac{\Sigma(F_i - \hat{F}_i)^2}{\Sigma(F_i - \bar{F})^2}$$

$$(5.3) \sigma_i = \frac{F_i}{A_{CS}}; (5.4) \epsilon_i = \frac{(d_i - d_0)}{d_0}; \& (5.5) A_{CS} = \bar{t} \times W$$

Tangent modulus and stiffness were the output variables, and both measures were taken with respect to a control variable of collagenase concentration. Thereafter, a one-way ANOVA was used to determine whether significant differences existed within the variable's main effect. Thereafter, if a significant difference was found for either parameter, bonferroni post-hoc analyses would be conducted to determine whether the differences existed in comparing different concentrations.

The same routine was incorporated for the other measured variables (ultimate stress and ultimate strain). Finally, these measures allowed one to objectively determine whether different concentrations of collagenase had a significant effect on the mechanical properties of the TCL.

5.2.2 Results

5.2.2a Stress-strain curves

The initial testing results showed contrary findings to what was expected (Fig. 5.6). Specimen 1 was taken from the left-unknown hand; its stress-strain curves revealed unexpected results when treated with varying concentrations of collagenase (Fig. 5.6(a)). Overall, the strip treated with 500 units was shown to have the largest tangent modulus; whereas, the strip treated with 1000 units displayed the largest, ultimate stress along with the largest, ultimate strain (Fig. 5.6(a)). Contrasting results were found from testing the TCL from the right-unknown hand in which multiple strips were treated with the same concentrations of collagenase (Fig. 5.6(b)). Overall, the concentration of 500 units again exhibited the largest tangent modulus and had the largest ultimate stress; in contrast, the control strip was shown to have the largest ultimate strain (Fig. 5.6(b)). Again, varying results were found for the third TCL specimen which was taken from a right hand within our lab (Fig. 5.6(c)). The strip, treated with 1000 units of collagenase, was computed to have the largest, tangent modulus and the largest, ultimate stress while the strip, treated with 1250 units of collagenase, was found to have the largest, ultimate strain (Fig. 5.6(c)).

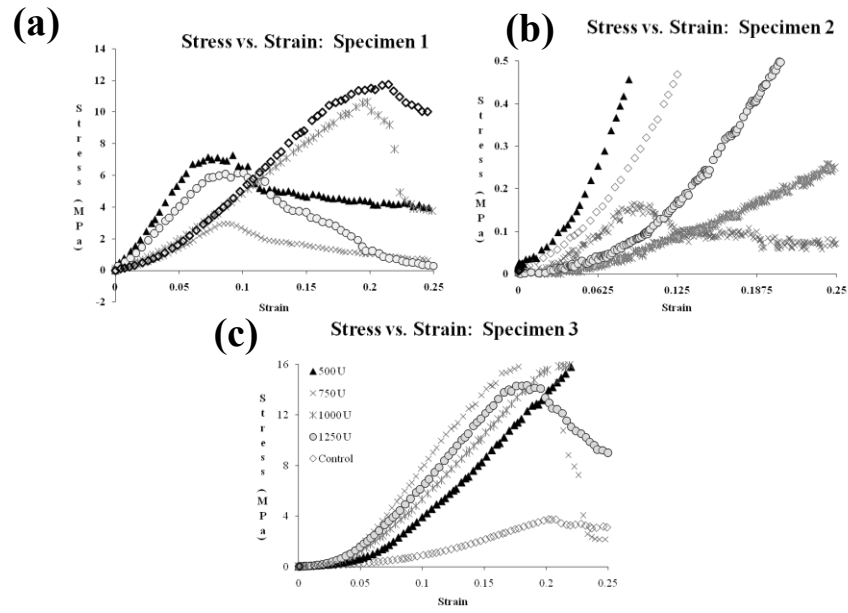


Figure 5.6. Displays stress-strain curves of the various treated transverse carpal ligaments in (a) an unknown left hand, (b) an unknown right hand, and (c) a right hand dissected within our lab.

5.2.2b Mechanical properties

Overall, the mechanical properties demonstrated the same varying results that were indicated by the TCL samples' stress versus strain curves (Figures 5.7, 5.8, 5.9, & 5.10). The tangent modulus was found to be the largest for the TCL samples that were treated with 500 units of collagenase; whereas, the tangent modulus of additional groups appeared in the following order with regards to their respective magnitudes: 1250 U, 750 U, 1000 U, and the placebo (Fig. 5.7). Statistical testing further verified the unexpected results where no differences were found ($P = 0.807$).

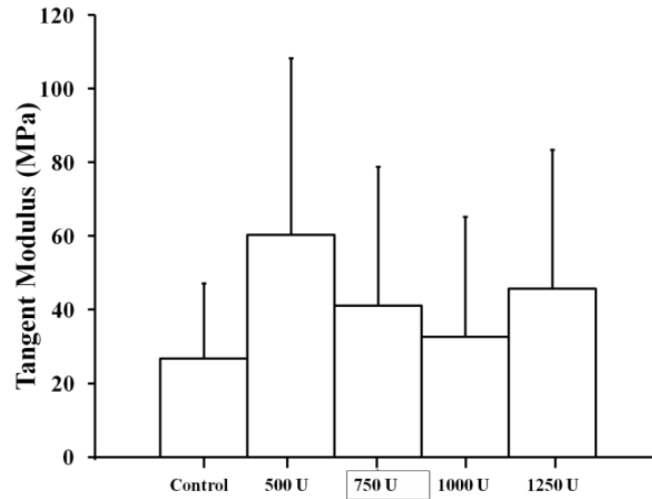


Figure 5.7. Displays the average tangent modulus where the statistics were computed across the three samples that were tested for each concentration.

Stiffness results echoed the similar pattern of irregularity that existed within the findings for tangent modulus (Fig. 5.8). However, contrasting results were found with regards to the respective order of average stiffness; whereas, the groups of TCL samples treated with 1250 U had the largest magnitude of stiffness in which additional magnitudes adhered to the following order: 500 U, 1000 U, placebo, and 750 U. The p-value was calculated to be non-significant with regards to the concentration of collagenase and its effect on the TCL's stiffness ($P = 0.831$).

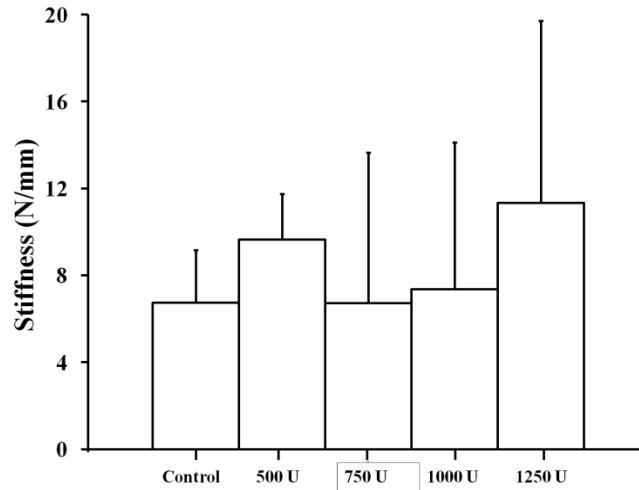


Figure 5.8. Shows the group stiffness (N/mm) trend with regards to the amount of collagenase.

The results for ultimate strain coincided with previous results in which unexpected averages were found (Fig. 5.9). Overall, the concentration of 1000 U displayed the smallest magnitude of ultimate strain followed by samples treated with 750 U, placebo, 500 U, and 1250 U of collagenase (Fig. 5.9). Statistical analysis showed no differences among the different groups of collagenase ($P = 0.567$).

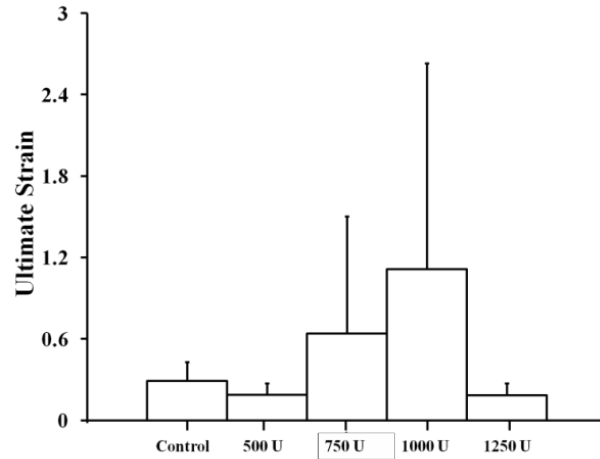


Figure 5.9. Reveals the trend of ultimate strain with regards to the concentration of collagenase.

The unexpected results were, again, echoed for the parameter of ultimate stress where an irregular pattern was found (Fig. 5.10). Overall, the group treated with 1000 units of collagenase exhibited the largest magnitude of ultimate stress followed by groups treated with 500 U, 1250 U, 750 U, and the placebo. Differences across groups were calculated to be non-significant ($P = .966$).

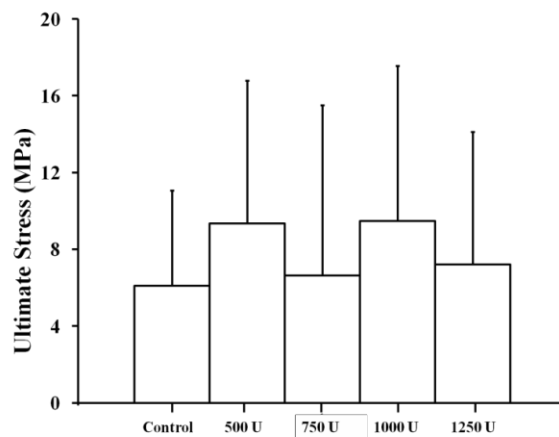


Figure 5.10. Average values for ultimate stress are shown with regards to the different groups of concentration and the respective control group.

5.3 EXPERIMENT 2: SUBMAXIMAL TESTING

5.3.1 Adjustments

5.3.1a Repeated measures design

In general, the same methodology that was implemented in the first experiment was utilized for the second experiment; however, several limitations were addressed in an attempt to monitor only the enzyme's effect on the ligament's mechanical and structural properties. Therefore, subsequent concerns for testing design were addressed individually in an attempt to account for the proximal-distal differences of the mechanical properties and to keep such properties consistent.

The second experiment was aimed to see whether collagenase was actively degrading the mechanical properties of the TCL. In the original attempt, testing design didn't account for the variable mechanical properties that existed along the proximal-distal length of the transverse carpal ligament. Emphasis was placed on eliminating such disparities. The proximal-distal midline of one TCL was found where two, subsequent samples were removed with two-millimeter widths. Both of these samples were taken two-millimeters proximally and two-millimeters distally from the proximal-distal midline. This attempt was aimed at choosing the ideal concentration of collagenase for treatment by judging its efficacy in degrading the TCL sample. The proximal segment was treated with 600 U while the distal segment was treated with 1200 U. In order to test the tissue repeatedly, the mechanical testing protocol had to be designed to load the tissue within its respective linear region while not causing irrecoverable damage.

5.3.1b Sub-maximal testing protocol

Testing efforts utilized a sub-maximal protocol (which is shown in figure 5.11) which allowed each sample to be repeatedly tested. Testing parameters were chosen based off of the previous results found from preceding experimentation while also considering past research. This allowed for the sample to be compared to its control properties in which the aforementioned methods attempted to keep the ligament strips' control properties consistent.

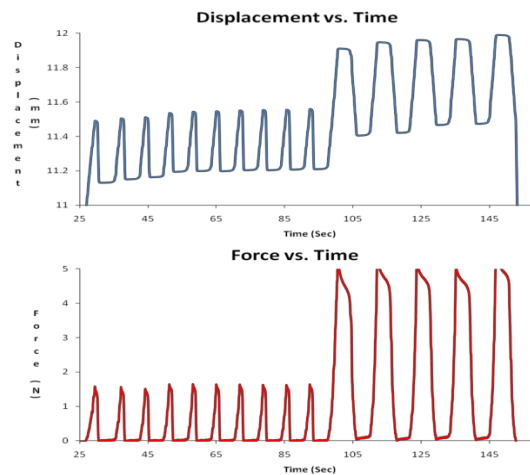


Figure 5.11. Shows an example testing protocol that was utilized in testing an actual ligament sample as well as all samples which developed based of Rowe et al. ⁽⁶²⁾

The protocol consisted of ten preconditioning cycles and five testing cycles where the displacement rate was held constant at 0.25 mm/s for both phases; however, load limits differed in that 1.5 N was used for each preconditioning cycle while 5 N was used for each testing cycle. Preconditioning was changed because past results consisted of several samples failing during the precondition phase which is why a lower load limit had to be implemented.

5.3.2 Results

The subjected samples of the transverse carpal ligament revealed small changes before and after treatment. Variable properties were for both segments where the proximal segment showed increases in stiffness and tangent modulus while the distal segment displayed decreases for both properties (Figures 5.12 and 5.13).

Control measurements showed that both the proximal and distal samples had similar stiffness magnitudes (Fig. 5.12). However, in response to collagenase, the distal segment revealed a decrease after being treated with 1200 units of collagenase while the proximal segment surprisingly increased with a slightly higher magnitude than its respective control after being treated with 600 units of collagenase (Fig. 5.12). Contrasting results were found upon accounting for the effect that collagenase had on each sample's tangent modulus.

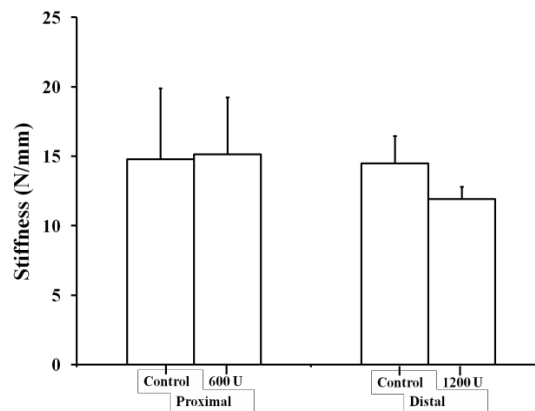


Figure 5.12. The stiffness results are shown where the control and the treated proximal segment is positioned on the left end while the control and the treated distal segment is positioned on the right end of the graph.

Proximal and distal segments showed contrary results for their respective, control measurements of tangent modulus (Fig. 5.13). An overall comparison between both segments showed that the proximal segment had a greater magnitude of tangent modulus than the distal segment in which the margin of difference was approximately 13 N. In response to collagenase,

contrasting results were, again, found for the proximal and distal segments. The collagenase concentration of 600 U stiffened the ligament by approximately 22 MPa; whereas, the other concentration of 1200 U decreased the distal segment by an approximate margin of 7 MPa.

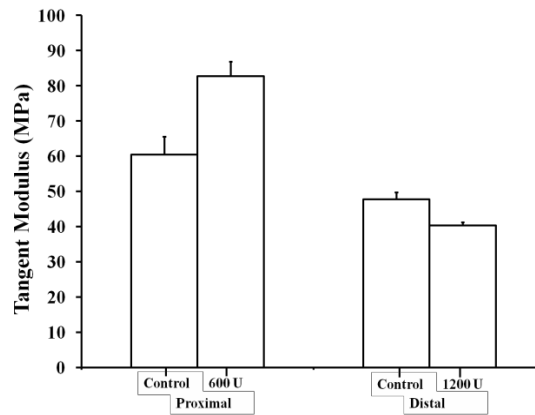


Figure 5.13. The results for tangent modulus are revealed where the control and the treated proximal segment is positioned on the left end while the control and the treated distal segment is positioned on the right end of the graph.

5.4 EXPERIMENT 3: TESTING AT ROOM TEMPERATURE

5.4.1 Adjustments

5.4.1a Collagenase preparation

The aforementioned method was used with one major caveat: each sample's respective treatment mixture was kept at room temperature. Additional changes also implemented an hourly testing effort where four samples were removed from one TCL specimen and tested before collagenase treatment as well as after each treatment hour for up to a total of four hours. However, in contrast to previous studies, only one concentration was used to treat each sample, 8000 U. Other changes consisted of developing an algorithm with MatLab® to analyze the average mechanical properties of each sample.

5.4.1b Parameter estimation

The algorithm was used to analyze resulting data from mechanical testing. Step 1 is revealed in the top left corner of figure 5.14; whereas, the data from testing is graphed for loading and displacement with both variables measured with respect to time. Thereafter, the algorithm allows for the user to pick the regions of interest within the mechanical testing protocol on the graph within the displacement versus time. The second step of the algorithm graphs the chosen region of interest with the loading points designated to the vertical axis while the corresponding, displacement points are designated to the horizontal axis. Two points were again picked to analyze the respective sample's stiffness (Eq. 5.1), maximum displacement, r-squared value (Eq. 5.2), and maximum force.

The user measurements of initial length and cross-sectional area were inputted within the command prompt to compute stress and strain values to display its curve of the respective, ligament sample (Eq. 5.3 and 5.4); whereas, cross-sectional (CS) area was, again, considered rectangular (Eq. 5.5).

Further analysis was done along with the stress versus strain computations where the maximum stress and maximum strain were simultaneously calculated. Tangent modulus was computed after the user had picked two points to signify the region of interest. Based upon this region, similar calculations were completed to compute the tangent modulus and its respective r-squared value. This process was completed for each testing cycle in which parameter averages were used for mean hypothesis testing for each parameter.

MatLab® Algorithm

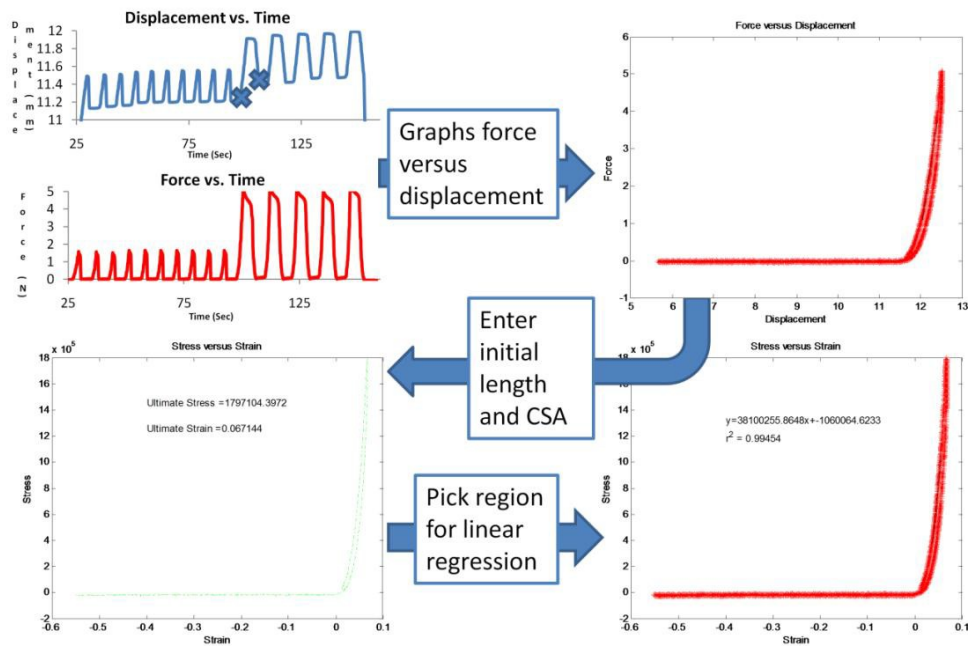


Figure 5.14. Highlights the general process used to analyze the mechanical properties for each ligament sample.

Parameters of interest (stiffness, tangent modulus, and maximum strain) were each subjected to a one-factor repeated measures analysis of variance (ANOVA). If an overall difference was found, bonferroni post-hoc analyses were done to determine where such differences were found.

5.4.2 Results

The repeated measures design was maintained for each TCL sample throughout the four hours of treatment duration where aforementioned measurements were made before treatment and after each hourly increment of treatment. Overall, each parameter of interest showed marginal differences among the control and subsequent treatment groups ($P > 0.05$).

Thickness estimates were measured six times for each sample before and after each hour of treatment. Average thickness for all six estimates is shown for each sample and its corresponding treatment duration (Fig. 5.15). Observing such values reveal a decreasing trend that indicated enzymatic degradation (Fig. 5.15). However, parameters of interest failed to show such activity.

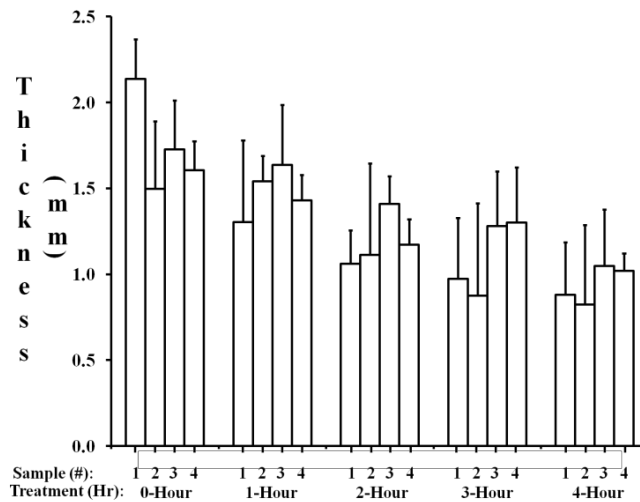


Figure 5.15. Displayed above is the average thickness measured for each TCL sample before collagenase treatment and after each hour of treatment.

Stiffness was also measured and averaged across all five testing cycles (Fig. 5.16). Similar to the measured thicknesses, a decreasing trend was found for stiffness in comparing the different treatment groups to the control; however, in contrast to thickness results, the overall difference between the control and the fourth hour of treatment was found to be marginal (Fig. 5.16). The average stiffness for the control group was found to have the largest magnitude with an approximate value of 12 N/mm (Fig. 5.16). The magnitude of the percent change was estimated to be approximately 11% where other percent changes were found to be smaller. These marginal differences were found to be non-significant ($P = 0.84$).

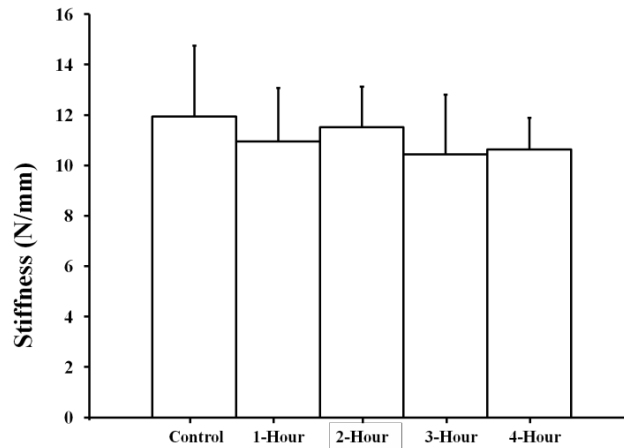


Figure 5.16. Shown in the above diagram is the average stiffness calculated among the tested TCL samples before collagenase treatment and after each hour of treatment.

Contrary to the stiffness results, normalizing force with the respective ligament’s cross-sectional area and accounting for strain showed an increasing trend in response to the increasing time duration of the treatment for the respective, ligament samples. Such trend observations were also indicated by the tangent modulus results where the fourth hour of treatment showed the largest magnitude (Fig. 5.17). The fourth hour of treatment had the largest magnitude, ~55 MPa; while the control group was determined to have the smallest magnitude, ~32 MPa (Fig. 5.17). Overall, a non-significant difference was found in comparing all treatment groups ($P = 0.10$).

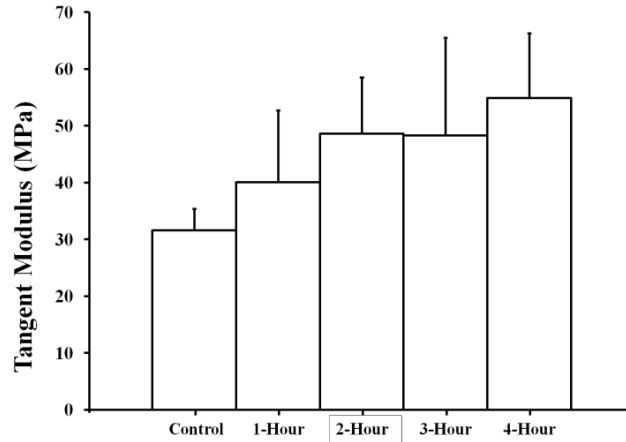


Figure 5.17. Depicted in the above diagram is the calculated trend between treatment duration and the average tangent modulus.

Maximum strain was considered for each cycle of the testing phase; the averages are shown in figure 5.18. The third hour of treatment had the largest magnitude, 0.078; whereas, the preceding hour of treatment revealed to have the smallest magnitude of maximum of strain, 0.059 (Fig. 5.18). However, no observable trend can be determined (Fig. 5.18). Furthermore, statistics determined that such group differences were infinitesimal, and a non-significant difference was found from the repeated measures analysis of variance ($P = 0.41$).

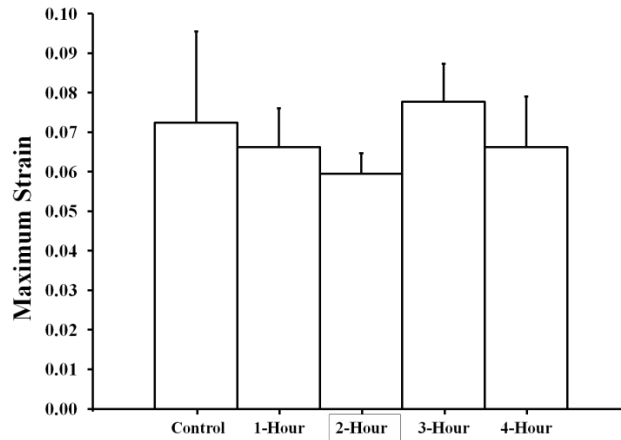


Figure 5.18. Outlines the relationship between maximum strain and treatment duration where testing was sub-maximal with a load limit at 5 N.

Figure 5.19 shows each hour of collagenase treatment and its hourly effect on one of the four ligament samples. Please note that control pictures were not taken where comparative observations cannot be made with its original state. One general observation that can be inferred is that fiber debridement seemed to occur while the sample was treated (Fig. 5.19). However, this observation is speculative because one cannot compare the experimental groups to the original.

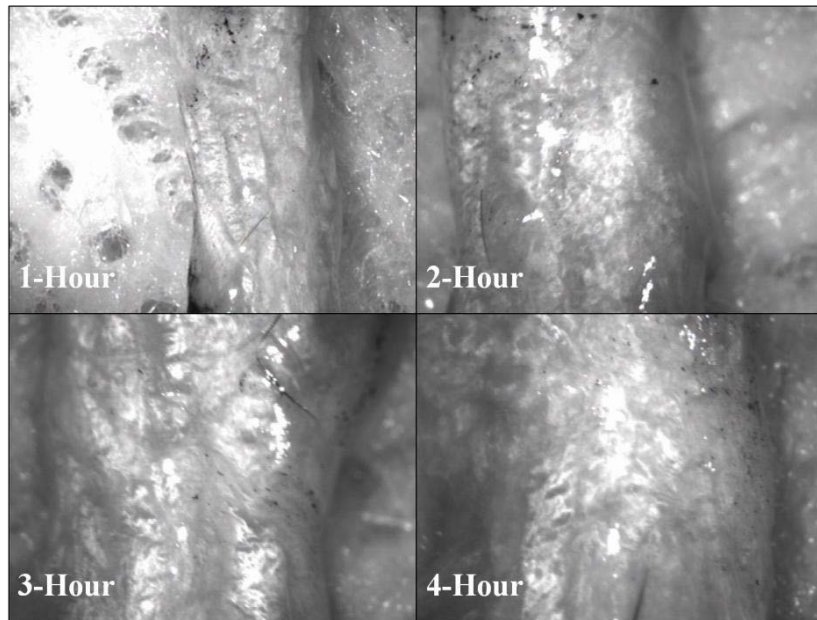


Figure 5.19. Displayed in the above picture are the microscope pictures that were taken for the ligament sample after 1-hour, 2-hour, 3-hour, and 4-hour of treatments.

5.5 DISCUSSION

5.5.1 Experiment 1

Overall results were found to be unexpected while not conferring with the original hypothesis. The overall, unexpected results could have stemmed from the inactivity of collagenase because results from the experimental procedure showed to be insufficient. Additional explanation could stem from the possible variability of its mechanical properties which was indicated by past research showing the TCL having different values of thickness ranging from 1.3 to 3.0 mm.⁽⁷²⁾

With regards to the mechanical properties for any soft tissue, types I and III collagen are known to bear significant portions of the load.⁽⁴²⁾ Chung et al found that both types of collagen are homogeneously distributed throughout the proximal-distal length of the TCL for the non-pathological ligament. However, this testing showed no difference within the mechanical properties of the TCL after subjecting each strip to a different concentration of collagenase.

Additional reasons for these contrary results could also stem from the inhomogeneity of mechanical properties within different areas of the TCL; however, little experimentation has proven the existence of such differences. Since type I collagenase non-specifically degrades the alpha helix sub-type of collagen, then, the prepared concentrations of the enzyme weren't active throughout the treatment of three hours because the mechanical properties of the treated versus the untreated showed no differences ($P > 0.05$). Thus, several adjustments needed to be made in order to properly test the TCL.

Testing concerns that pertained to the lack of collagenase activity were the solution's temperature while the possible inhomogeneity of mechanics for the TCL also posed additional concerns. In addition, limitations were found within the used specimens where, in particular, the two unknown cadaver arms were not documented well. Thus, little knowledge was known on the specimen prior to experimentation. However, it was clear that one specimen, in particular, acted as an outlier case; more specifically, the right unknown specimen showed drastically compromised properties in response to collagenase. But, such deficits in properties could also be the results of additional, outside factors. Therefore, several adjustments were made to account for these limitations before testing recommenced.

5.5.2 Experiment 2

The calculated properties, again, indicated variable results. The proximal segment's stiffness exhibited a small increase in response to 600 units of collagenase while a more drastic increase was computed for its tangent modulus. However, the distal segment's properties decreased in response to 1200 units of collagenase. Therefore, these results, again, raise the question to whether collagenase was active throughout each segment's treatment duration because its efficacy on the TCL's proximal segment was counterintuitive.

My experimental efforts, again, proved to have their limitations where I could not quantitatively determine the effectiveness of collagenase. However, these non-uniform results made me believe that the enzyme wasn't active throughout the ligament's treatment. This was observed because I accounted for the control mechanical properties of each ligament sample; whereas, both samples had similar control stiffness values. In contrast, the proximal segment's tangent modulus was shown to be approximately 2 times the size of the distal segment; their respective, control values of stiffness showed a smaller margin of difference. Therefore, counterintuitive findings resulted even with the current, repeated measures design which allowed for the account of regional differences between segments. Further observation of the results has led to the belief that putting each mixture or each test-tube on ice has had a significant effect on the activity of the enzyme.

5.5.3 Experiment 3

My repeated measures design allowed for seeing whether collagenase was actively degrading the ligament's collagen while also determining its time dependent response. However, contrasting findings were found with regards to the stiffness results in which a non-significant difference was found among the different groups of treatment duration and their respective control values. Statistics further prove that the collagenase was relatively inert. In the same vein, the addition of collagenase was shown to increase the TCL's tangent modulus; however, statistics didn't verify this conclusion in areas where such differences were determined to be non-significant. Similar conclusions can also be said about the maximum strain where, again, a non-significant difference was found. Therefore, based upon the results, experimental limitations were, again, causes for concern because of our counterintuitive results. Thus, it would be best to revisit past methodologies to determine several experimental factors involved within activating bacterial-derived collagenase. ^(6, 8, 62)

6.0 COLLAGENOLYTIC CHANGES TO THE TCL'S TENSILE PROPERTIES

6.1 VARIABLES AFFECTING COLLAGENASE

Several of the past studies that we revisited consisted of looking at collagenase's effect on pathogenic chords, rat periodontal ligaments, and rat diaphragm muscle. ^(6, 8, 62) Among the aforementioned studies, several of them shared common features in their preparation methodology; but they also exhibited contrasting features that were concerning. ^(6, 8, 62)

Differentiating characteristics were mostly isolated within current research completed on pathogenic chords. These differences extend from the fact that these studies involve treating an in-vivo pathology; whereas, most of the subsequent research looked into its effects with regards to an uncontrolled environment or the human wrist. Please note that such findings greatly apply to the research where the pathogenic chords are mainly located within the hand and, at the same time, proximal to the concerning TCL anatomy. ⁽⁴⁸⁾

Additional differences existed within their method of enzyme distribution, injection. The time of treatment also varied as well for several in-vivo studies. ^(47, 48) However, Starkweather et al did control for temperature and time of distribution; such chords were subjected to 24 hours of treatment at body temperature. Other similarities found in comparison to my study included the tissue's type of collagen; pathogenic chords were made up of type I and III collagen which makes up the majority of load bearing constituents within the TCL. ⁽⁶⁾

The rat periodontal ligament was also determined to be made up of a majority of type I and III collagen. ⁽⁶⁵⁾ However, contrary to past research on pathogenic chords, these studies implemented a medium of enzyme treatment that immersed the ligament which coincided with my study. ⁽⁸⁾ Similar to my study, each ligament was treated continuously for four hours.

Contrasting characteristics to my study included the implemented type of collagenase, type III, and its set temperature for each solution, 37 °C. ⁽⁸⁾ In addition, this study also used a bio-shaker or incubator to constantly disturb the medium of each mixture as well as a phosphate buffered saline (PBS) solvent to activate collagenase activity. ⁽⁸⁾

The main similarities that were found between the study on rat diaphragm muscle and my study was the usage of collagenase on a tissue for a series of repeated measurements of the mechanical properties with a sub-maximal, mechanical protocol for testing. ⁽⁶²⁾ Their sub-maximal testing protocol was actually incorporated within our experimental design. However, existing differences between both studies were the five minute duration of treatments where each tissue strip was subjected to collagenase for a total 25 minutes of collagenase as well as the tissue's type of collagen where the main collagen constituents were type IV in addition to type I and III. ⁽⁶²⁾ Other differences consisted of implementing type II collagenase, setting the treatment solution at 37 °C, and using Rees-Simpson solution. ⁽⁶²⁾

Past studies of collagenase's effect on soft tissues' mechanics regularly used different solvents and solution temperatures. Further examination of a past study led to finding several factors that bear significant importance in activating collagenase: calcium molarity, temperature, and pH level. Woessner et al determined that, in order to activate collagenase, a calcium molarity of 0.01 M is required; whereas, in my experiment, I used a calcium molarity that was less than 1.0×10^{-4} M. ⁽⁶⁶⁾ Therefore, my methodology needed to purchase a buffer with a larger concentration of calcium. In addition, Woessner et al also tested collagenase activity with respect to temperature, or more specifically the range from 30 °C to 37 °C. ⁽⁶⁶⁾ Subsequent observations of collagenase activity found that the enzyme attacked collagenase at 30 °C; however, it failed to release common by-products indicative of collagenase digestion. ⁽⁶⁶⁾ In

contrast, when the temperature was raised to 37 °C, the aforementioned researchers found that those common by-products were released. In comparison, I kept my solutions' temperatures ranging somewhere above freezing temperature to room temperature (5 °C - 25 °C). Therefore, such treatment was ineffective throughout the allotted four hours; and this was also verified when the statistical decreases within the mechanical properties couldn't be discerned within past results. Finally, an observation was made that optimal collagenase activity existed when the used solvent's temperature was approximately 7.5 pH. ⁽⁶⁶⁾ A buffer that was found to have a pH range from 7.2 – 7.5 was implemented and led to the belief that the pH level wasn't as much of a concern as temperature and calcium molarity. Therefore, consideration of the aforementioned factors made me reconsider several variables of my current design.

6.2 EXPERIMENTAL DESIGN: ADJUSTMENTS

Several adjustments were made to the original methodology: temperature, continuous agitation of the solvent, and collagenase solvent. All of which concerned the original collagenase preparation. Temperature and continuous agitation concerns were addressed with the use of a bench-top shaker (Fisher Scientific; Pittsburgh, PA) which was maintained at 37 °C. Collagenase solvent problems were solved by using 10X Hank's Balanced Salt Solution (HBSS) (Invitrogen; Carlsbad, CA) which had large molarity of calcium chloride, ~0.013 M.

Multiple samples were divided from a TCL specimen removed from a cadaver hand. After careful dissection and removal, the TCL was divided into nine total samples in which all were roughly standardized to have 2 mm widths. The treatment phase consisted of successive hourly durations within a treatment medium; each sample was placed in a separate petri dish with approximately 1500 U of collagenase and 2 mL of HBSS. Nine dishes were constantly agitated with a bench-top shaker while each solution's environment was kept at 37 °C.

Mechanical testing, precede measurements to each treatment hour as well as after the third hour of treatment, and data reduction consisted of the same protocol as previous experiments. However, in the case of a failure during the testing cycles, both measurements were computed by using a range of 30% of the maximum to the maximum force or stress. If a sample failed during pre-conditioning, the value was treated as zero. A one-way ANOVA was performed to compare changes in stiffness and tangent modulus. The significance level was $p < 0.05$.

6.3 RESULTS

Figure 6.1 displays representative force versus displacement curves of a ligament sample. In general, the control sample shows a steeper slope than the other treatments. The slopes of the 1- and 2-hour treatments were found similar. After the 3-hour treatment, the sample failed well below the force limit of 5 N during the testing. Not every force versus displacement curves displayed these characteristics; however, a majority of the failure cases represented this loading behavior before and after each treatment hour.

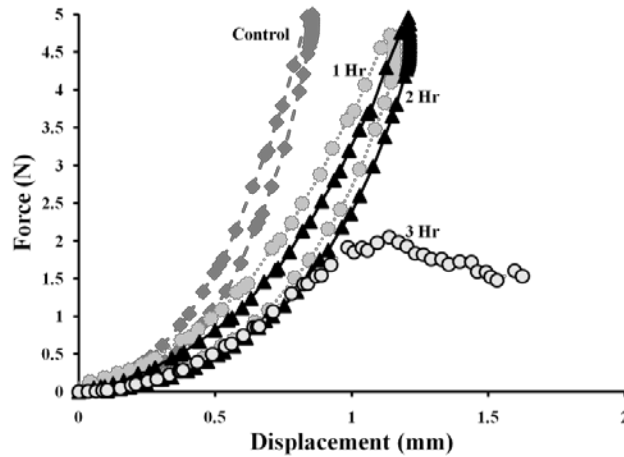


Figure 6.1. Representative displacement-force curves of a sample.

Sample failures were variable. Table 6.1 shows if and when each sample failed during the experiment. Three samples never failed for the 3-hour treatment. No sample failed after the 1-hour treatment. One sample failed after the 2-hour treatment. After 3-hour treatment, a majority of samples (N = 5) failed during either preconditioning or testing indicating a critical point within this treatment duration.

Table 6.1. Failure time point (×) of each sample.

Treatment Duration	Sample	1	2	3	4	5	6	7	8	9
2-Hour	Preconditioning									
	Testing						×			
3-Hour	Preconditioning	×								
	Testing			×		×		×		×

Collagenase treatment significantly affected the stiffness of the ligament ($p < 0.001$; Fig. 6.2). Post- hoc pair-wise comparisons showed there were no significant differences among the control, one-hour and two-hour treatment samples. However, the control group's average

stiffness was observed to have the largest magnitude, 11 N/mm (Fig. 6.2). The stiffness after the third hour of treatment was significantly lower than any of the other groups. The 3-hour treatment reduced the stiffness by 64% in comparison to the controls (Fig. 6.2).

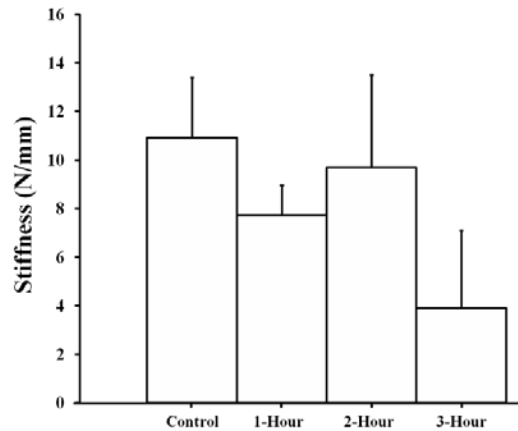


Figure 6.2. Stiffness with different treatment durations.

The treatment duration of collagenase didn't significantly impact the ligament's tangent modulus ($p > 0.05$; Fig. 6.3). Further comparison of each group's average tangent modulus revealed that the second hour of treatment had the largest magnitude, 50 MPa (Fig. 6.3). General observation showed no distinguishing trend within the graph which was also indicated by the non-significant difference found within the statistical test ($p < 0.05$).

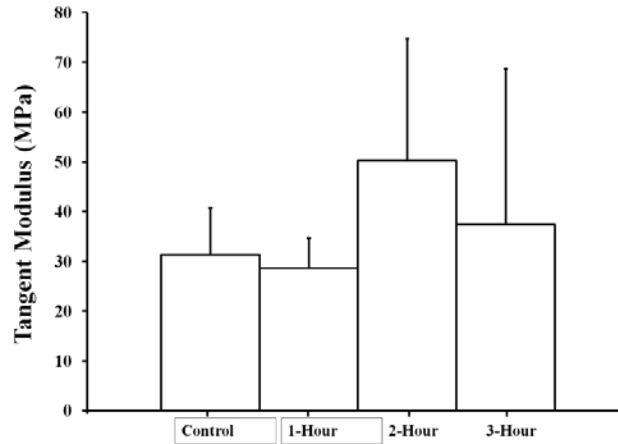


Figure 6.3. Tangent modulus with different treatment durations.

TCL samples regularly exhibited fiber debridement which is shown within the figure below; the third hour of treatment appeared more uneven in comparison to the control sample's area. Other commonly seen characteristics indicated an irregular fiber pattern as well as fiber loosening; whereas, one can visually see the general alignment of the fibers for the control while, for the sample treated three hours, no fiber alignment could be deduced. However, such degradation wasn't quantified; whereas at the time, these observations were difficult to distinguish among other samples as some people may infer from the observational results for the second sample.

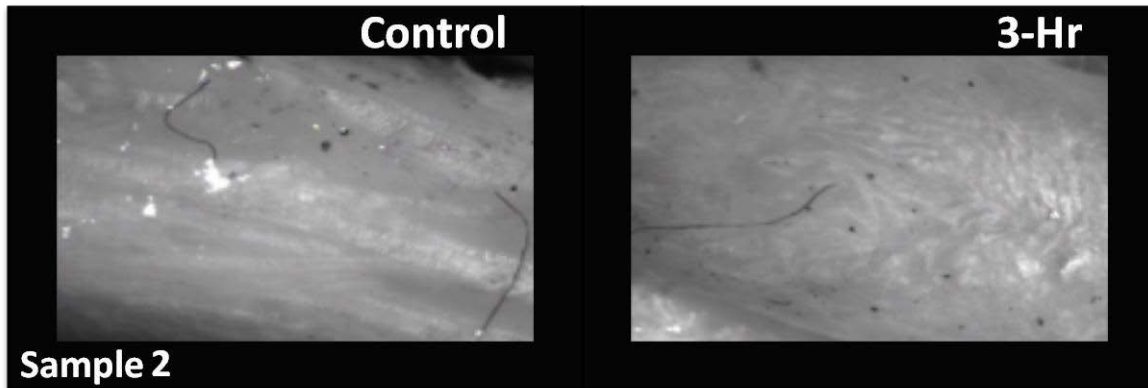


Figure 6.4. Shown above are the common visual changes that are seen within the second TCL sample before and after treatment.

6.4 DISCUSSION

6.4.1 Collagenase activity

Validation of my findings consisted of determining whether the calculated stiffnesses for all TCL samples within the control were comparable; comparison was evident where stiffness varied from 7.3 to 15.4 N/mm. In addition, a power analysis was done to determine the significant effect for a paired t-test corrected for the four comparisons. Average and standard deviation for the control stiffness values were used to determine the required sample size while $\alpha = 0.0083$ and power = 0.91. Results showed that a sample size of six is sufficient in order to determine a significant effect; whereas, nine samples were used within this experiment. Therefore, I can reliably say that collagenase could effectively reduce the stiffness of the TCL. In particular, the third hour of treatment reduced ligament stiffness by more than 50%. However, the similar stiffness values that were shown for the control and the first as well as second hour of treatment suggest that it takes more than two hours for the collagenase to alter effectively the mechanical properties of the ligament. In

contrast, the gradual change formerly shown in other tissues to stiffness couldn't be found. Therefore, the insensitivity of stiffness to collagenase during the first two hours of treatment may be, again, explained by external factors in the solvent that weren't accounted.

The collagenase mixture used in this study contained a large concentration of dextrose, which can cause cross-linking to form among a soft tissue's collagen fibers.⁽⁶⁷⁾ The cross-links tended to strengthen the tissue's mechanical properties and to neutralize the enzymatic degradation during the first two hours of treatment.⁽⁶⁸⁾ As treatment duration increased, the efficacy of collagenase became more apparent as individual collagen fibers approached fracture. No changes in average modulus were found when comparing across different treatments; this further validates the offsetting effect of dextrose.

Additionally, we found that the tangent modulus for the TCL didn't change with regards to treatment duration. Reasoning for these results could have also surmised because of the addition glucose as well as other salts; whereas, the hourly treatment could have not only activated collagenase but also created a hypertonic solution for each sample. Such effects could potentially complicate results where the surrounding fluid's osmolarity was found to cause significant differences with regards to a ligament's mechanical properties by effectively decreasing its cross-sectional area through water exuding out of the tissue.⁽⁷¹⁾ Furthermore, the HBSS buffer used to activate collagenase contained an osmolarity of approximately 3.0 osm while the tissue maintained an osmolarity of 0.3 osm. This created a hypertonic solution and dehydrated the tissue while immersing it within the buffer. Past research has shown that such dehydration to the medial collateral ligament may cause increases in the ligament's stiffness with changes in the tissue surrounding osmolarity of as little as 1.80 osm.⁽⁷¹⁾ Therefore, since our

surrounding osmolarity was 3.0 osm, significant changes could have been induced within each ligament sample causing unexpected increases in its mechanical properties as well as its stiffness due to subsequent dehydration.

Therefore, I can't say that tangent modulus wasn't significantly affected by the inclusion of collagenase because additional factors, such as dextrose and the buffer's osmolarity, could have modulated the TCL's microstructure either chemically or physically. Therefore, additional studies should look into controlling such factors or effectively eliminating them. Such elimination could elucidate changes within the TCL's stiffness as well as its mechanical properties.

6.4.2 Future studies

Future studies should incorporate a solvent without dextrose, different collagenase concentrations, and more variable time points. The TCL consists of a significant amount of different types of collagen; therefore, additional studies could also incorporate a mixture of different types of collagenase that target these types of collagen. In addition to these findings, types I and III collagen weren't quantified with an accepted imaging modality, thereby, collagenolytic activity couldn't be proved. Future direction should use imaging to validate collagenolytic activity before subsequent mechanical testing is pursued.

Additionally, collagenase could be possibly used as therapeutic agent in treating carpal tunnel syndrome; however, several additional procedures would have to be incorporated. Recent research has looked into using carpal tunnel balloon plasty (CTBP) as an alternative to carpal tunnel release ⁽³⁹⁾; whereas, the inclusion of collagenase could effectively facilitate CTBP to stretch and induce permanent deformation within the TCL and to allow for the median nerve to decompress. Similarly, other studies have looked into collagen's ability to act as a smart

material. Ruberti et al used bovine, corneal tissue to determine if the collagen behaves in such a manner. ⁽⁶⁰⁾ What they proved is that collagenase's ability to degrade tissue was diminished when strain was induced within the tissue where collagen aligned blocking possible substrates for the situated collagenase. ⁽⁶⁰⁾ Such observations were determined with an image-based research which observed the tissue's birefringence pattern resulting from polarized microscopy. Thus, if this response is shown within the TCL's collagen architecture, utilizing active collagenase with the TCL in a relaxed state might prove to be fruitful in treating carpal tunnel syndrome. Li et al. have shown that carpal bone rotation may be induced within the hamate and the trapezium. ⁽³⁹⁾ Therefore, subsequent rotation may create a relaxed state within the TCL and allow for collagenase to actively degrade the collagen substructure of the ligament. However, such observations are speculative; whereas, more studies need to be done in order to determine if such interactions occur.

7.0 CONCLUSION

My experimental aims were focused to quantify the preferential directions within the TCL's collagenous network as well as to determine the efficacy of collagenase in degrading the TCL's respective soft tissue mechanics. Small angle light scattering was employed in isolating the transverse carpal ligament's fiber orientation. In addition, after several experimental attempts, I did find that collagenase can alter the structural properties of the TCL. Thus, collagenase can be used to effectively lengthen the TCL and could possibly be implemented as an alternative treatment for carpal tunnel syndrome instead of carpal tunnel release.

Observations of the collagen fiber arrangement within the TCL have proven to be contradictory. Small angle light scattering (SALS) has been effectively employed to determine the preferential directions of various soft tissues to a quantitative degree of accuracy. Reference state orientation was determined for different depths of the TCL. Angular dispersion was found to differ non-significantly with respect to the TCL's depth where either depth could be used to represent the angular frequency plot for the ligament and be used to model the reference configuration of the TCL.

The fiber percentages determined that the preferential directions within the TCL were concluded to adhere to the following arrangement in terms of prominence: transverse, pisiform-trapezium oblique, scaphoid-hamate oblique, and longitudinal. Furthermore, differences were found to be very significant ($P < 0.0001$) and indicated an overall majority of fibers within the TCL directed in the transverse directions. Such observations may also infer the ligament's physiology within the carpal tunnel. Furthermore, insights from other studies infer directionality within the function of the carpal tunnel as well as the ligament's significance with regards to its function. Such studies indicate contrasting results for its function in carpal tunnel stability.

However, the majority of transverse fibers within the TCL may indicate its capacity to stabilize its respective insertion sites transversely; they also indicate its importance in preventing changes within carpal tunnel anatomy as well as preventing carpal tunnel contents from traveling in the palmar direction.

Carpal tunnel release has shown to cause several post-operative complications, regardless of the type of surgery. Thus, alternative options should be developed to reduce the risks of carpal tunnel release. Few studies have researched the TCL's mechanical properties where no one has addressed its properties subjected to enzymatic degradation. Initial attempts to determine the influence of collagenase on the mechanical properties proved to be fruitless with regards to my aims; however, they eventually led to the development of a proper experimental procedure. The subjection of collagenase to several TCL samples led to subsequent decreases to their stiffness after three hours of treatment; however, a trend couldn't be discerned between the time of subjection and the TCL samples' stiffness. In addition, external factors existing within the buffer, such as dextrose and osmolarity, might have led to the non-conventional trend between time of subjection and stiffness; whereas, dextrose, which could act as a strengthening agent, has been known to induce cross-linking within a ligament. Similarly, differences between the osmolarities of the tissue and its surrounding solvent could have dehydrated the tissue and effectively increase its mechanical and structural properties. Future studies should look into using a buffer without dextrose and with a low osmolarity while implementing other types of collagenase. Future studies should look into using a buffer without dextrose while implementing other types of collagenase.

In closing, such research with regards to the TCL collagen network's orientation and to the mechanical deficit created by enzymatic degradation may potentially provide for a viable alternative to the current treatment option. Additionally, such structural measurements may lead to a more accurate computational model for the TCL following the constitutive relationship

utilized by Lanir et al and Sacks. Furthermore, these research efforts may lead to the development of a treatment that avoids the occurrence of post-operative complications by altering the TCL's load bearing constituents allowing for the ligament to deform or to be elongated with a mechanical stimulus. Finally, this treatment option would have to allow for the ligament to be effectively functional while compromising the TCL's stiffness.

BIBLIOGRAPHY

1. Pavlidis L, Chalidis BE, Demiri E, Dimitriou CG. The effect of transverse carpal ligament lengthening on carpal tunnel volumetry: a comparison between four techniques. *Ann Plast Surg.* 2010;65(5):480-4.
2. Perumal S, Antipova O, Orgel JP. Collagen fibril architecture, domain organization, and triple-helical conformation govern its proteolysis. *Proc Natl Acad Sci U S A.* 2008;105(8):2824-9. PMID: 2268544.
3. Isogai S, Murakami G, Wada T, Akita K, Yamashita T, Ishii S. Lamina configuration of the transverse carpal ligament. *J Orthop Sci.* 2002;7(1):79-83.
4. Sacks MS, Smith DB, Hiester ED. A small angle light scattering device for planar connective tissue microstructural analysis. *Ann Biomed Eng.* 1997;25(4):678-89.
5. Goldfarb CA, Yin Y, Gilula LA, Fisher AJ, Boyer MI. Wrist fractures: what the clinician wants to know. *Radiology.* 2001;219(1):11-28.
6. Starkweather KD, Lattuga S, Hurst LC, Badalamente MA, Guilak F, Sampson SP, et al. Collagenase in the treatment of Dupuytren's disease: an in vitro study. *J Hand Surg Am.* 1996;21(3):490-5.
7. Komatsu K. Mechanical strength and viscoelastic response of the periodontal ligament in relation to structure. *J Dent Biomech.* 2010;2010. PMID: 2951112.
8. Komatsu K, Shibata T, Shimada A. Analysis of contribution of collagen fibre component in viscoelastic behaviour of periodontal ligament using enzyme probe. *J Biomech.* 2007;40(12):2700-6.
9. Buchanan D, Ural A. Finite element modeling of the influence of hand position and bone properties on the Colles' fracture load during a fall. *J Biomech Eng.* 2010;132(8):081007.
10. Troy KL, Grabiner MD. Off-axis loads cause failure of the distal radius at lower magnitudes than axial loads: a finite element analysis. *J Biomech.* 2007;40(8):1670-5.
11. Luria S, Hoch S, Liebergall M, Mosheiff R, Peleg E. Optimal fixation of acute scaphoid fractures: finite element analysis. *J Hand Surg Am.* 2010;35(8):1246-50.
12. Choi WJ, Robinovitch SN. Pressure distribution over the palm region during forward falls on the outstretched hands. *J Biomech.* 2011;44(3):532-9.
13. Guo X, Fan Y, Li ZM. Effects of dividing the transverse carpal ligament on the mechanical behavior of the carpal bones under axial compressive load: a finite element study. *Med Eng Phys.* 2009;31(2):188-94.

14. Sacks MS. Incorporation of experimentally-derived fiber orientation into a structural constitutive model for planar collagenous tissues. *J Biomech Eng.* 2003;125(2):280-7.
15. Gasser TC, Ogden RW, Holzapfel GA. Hyperelastic modelling of arterial layers with distributed collagen fibre orientations. *J R Soc Interface.* 2006;3(6):15-35. PMID: 1618483.
16. Rotman MB, Donovan JP. Practical anatomy of the carpal tunnel. *Hand Clin.* 2002;18(2):219-30.
17. Cobb TK, Dalley BK, Posteraro RH, Lewis RC. Anatomy of the flexor retinaculum. *J Hand Surg Am.* 1993;18(1):91-9.
18. Stecco C, Macchi V, Lancerotto L, Tiengo C, Porzionato A, De Caro R. Comparison of transverse carpal ligament and flexor retinaculum terminology for the wrist. *J Hand Surg Am.* 2010;35(5):746-53.
19. Ettema AM, Zhao C, An KN, Amadio PC. Comparative anatomy of the subsynovial connective tissue in the carpal tunnel of the rat, rabbit, dog, baboon, and human. *Hand (N Y).* 2006;1(2):78-84. PMID: 2526031.
20. Brooks JJ, Schiller JR, Allen SD, Akelman E. Biomechanical and anatomical consequences of carpal tunnel release. *Clin Biomech (Bristol, Avon).* 2003;18(8):685-93.
21. Chow JC, Hantes ME. Endoscopic carpal tunnel release: thirteen years' experience with the Chow technique. *J Hand Surg Am.* 2002;27(6):1011-8.
22. Amadio PC. The first carpal tunnel release? *J Hand Surg Br.* 1995;20(1):40-1.
23. Benson LS, Bare AA, Nagle DJ, Harder VS, Williams CS, Visotsky JL. Complications of endoscopic and open carpal tunnel release. *Arthroscopy.* 2006;22(9):919-24, 24 e1-2.
24. Okutsu I, Hamanaka I, Tanabe T, Takatori Y, Ninomiya S. Complete endoscopic carpal tunnel release in long-term haemodialysis patients. *J Hand Surg Br.* 1996;21(5):668-71.
25. Garcia-Elias M, An KN, Cooney WP, 3rd, Linscheid RL, Chao EY. Stability of the transverse carpal arch: an experimental study. *J Hand Surg Am.* 1989;14(2 Pt 1):277-82.
26. Fuss FK, Wagner TF. Biomechanical alterations in the carpal arch and hand muscles after carpal tunnel release: a further approach toward understanding the function of the flexor retinaculum and the cause of postoperative grip weakness. *Clin Anat.* 1996;9(2):100-8.
27. Xiu KH, Kim JH, Li ZM. Biomechanics of the transverse carpal arch under carpal bone loading. *Clin Biomech (Bristol, Avon).* 2010;25(8):776-80. PMID: 2919606.
28. Katz JN, Fossel KK, Simmons BP, Swartz RA, Fossel AH, Koris MJ. Symptoms, functional status, and neuromuscular impairment following carpal tunnel release. *J Hand Surg Am.* 1995;20(4):549-55.

29. Mirza MA, King ET, Jr., Tanveer S. Palmar uniportal extrabursal endoscopic carpal tunnel release. *Arthroscopy*. 1995;11(1):82-90.
30. Seradge H, Seradge E. Piso-triquetral pain syndrome after carpal tunnel release. *J Hand Surg Am*. 1989;14(5):858-62.
31. Hunter JM. Recurrent carpal tunnel syndrome, epineural fibrous fixation, and traction neuropathy. *Hand Clin*. 1991;7(3):491-504.
32. Wilson KM. Double incision open technique for carpal tunnel release: an alternative to endoscopic release. *J Hand Surg Am*. 1994;19(6):907-12.
33. Netscher D, Mosharafa A, Lee M, Polsen C, Choi H, Steadman AK, et al. Transverse carpal ligament: its effect on flexor tendon excursion, morphologic changes of the carpal canal, and on pinch and grip strengths after open carpal tunnel release. *Plast Reconstr Surg*. 1997;100(3):636-42.
34. Netscher D, Lee M, Thornby J, Polsen C. The effect of division of the transverse carpal ligament on flexor tendon excursion. *J Hand Surg Am*. 1997;22(6):1016-24.
35. Stevens JC, Sun S, Beard CM, O'Fallon WM, Kurland LT. Carpal tunnel syndrome in Rochester, Minnesota, 1961 to 1980. *Neurology*. 1988;38(1):134-8.
36. Hong CZ, Liu HH, Yu J. Ultrasound thermotherapy effect on the recovery of nerve conduction in experimental compression neuropathy. *Arch Phys Med Rehabil*. 1988;69(6):410-4.
37. Ebenbichler GR, Resch KL, Nicolakis P, Wiesinger GF, Uhl F, Ghanem AH, et al. Ultrasound treatment for treating the carpal tunnel syndrome: randomised "sham" controlled trial. *BMJ*. 1998;316(7133):731-5. PMID: 28476.
38. Horch RE, Allmann KH, Laubenberger J, Langer M, Stark GB. Median nerve compression can be detected by magnetic resonance imaging of the carpal tunnel. *Neurosurgery*. 1997;41(1):76-82; discussion -3.
39. Li ZM, Tang J, Chakan M, Kaz R. Carpal tunnel expansion by palmarly directed forces to the transverse carpal ligament. *J Biomech Eng*. 2009;131(8):081011.
40. Jakab E, Ganos D, Cook FW. Transverse carpal ligament reconstruction in surgery for carpal tunnel syndrome: a new technique. *J Hand Surg Am*. 1991;16(2):202-6.
41. Netscher D, Steadman AK, Thornby J, Cohen V. Temporal changes in grip and pinch strength after open carpal tunnel release and the effect of ligament reconstruction. *J Hand Surg Am*. 1998;23(1):48-54.
42. Woo SL, Debski RE, Withrow JD, Janaushek MA. Biomechanics of knee ligaments. *Am J Sports Med*. 1999;27(4):533-43.

43. Holmes MW, Howarth SJ, Callaghan JP, Keir PJ. Carpal tunnel and transverse carpal ligament stiffness with changes in wrist posture and indenter size. *J Orthop Res*. 2011.
44. Harper E, Berger A, Katchalski E. The hydrolysis of poly (L-Prolyl-Glycyl-L-Prolyl) by bacterial collagenase. *Biopolymers*. 1972;11(8):1607-12.
45. Rydevik B, Brown MD, Ehira T, Nordborg C. Effects of collagenase on nerve tissue. An experimental study on acute and long-term effects in rabbits. *Spine (Phila Pa 1976)*. 1985;10(6):562-6.
46. Badalamente MA, Hurst LC. Enzyme injection as nonsurgical treatment of Dupuytren's disease. *J Hand Surg Am*. 2000;25(4):629-36.
47. Badalamente MA, Hurst LC. Efficacy and safety of injectable mixed collagenase subtypes in the treatment of Dupuytren's contracture. *J Hand Surg Am*. 2007;32(6):767-74.
48. Hurst LC, Badalamente MA, Hentz VR, Hotchkiss RN, Kaplan FT, Meals RA, et al. Injectable collagenase clostridium histolyticum for Dupuytren's contracture. *N Engl J Med*. 2009;361(10):968-79.
49. Watt AJ, Curtin CM, Hentz VR. Collagenase injection as nonsurgical treatment of Dupuytren's disease: 8-year follow-up. *J Hand Surg Am*. 2010;35(4):534-9, 9 e1.
50. Sacks MS, Schoen FJ. Collagen fiber disruption occurs independent of calcification in clinically explanted bioprosthetic heart valves. *J Biomed Mater Res*. 2002;62(3):359-71.
51. McCally RL, Farrell RA. Small-angle light scattering and birefringence properties of chick cornea. *J Refract Surg*. 1999;15(6):706-10.
52. Hamann MC, Sacks MS, Malinin TI. Quantification of the collagen fibre architecture of human cranial dura mater. *J Anat*. 1998;192 (Pt 1):99-106. PMID: 1467743.
53. Debski RE, Moore SM, Mercer JL, Sacks MS, McMahon PJ. The collagen fibers of the anteroinferior capsulolabrum have multiaxial orientation to resist shoulder dislocation. *J Shoulder Elbow Surg*. 2003;12(3):247-52.
54. Nguyen TD, Liang R, Woo SL, Burton SD, Wu C, Almarza A, et al. Effects of cell seeding and cyclic stretch on the fiber remodeling in an extracellular matrix-derived bioscaffold. *Tissue Eng Part A*. 2009;15(4):957-63. PMID: 2787449.
55. Lake SP, Miller KS, Elliott DM, Soslowsky LJ. Effect of fiber distribution and realignment on the nonlinear and inhomogeneous mechanical properties of human supraspinatus tendon under longitudinal tensile loading. *J Orthop Res*. 2009;27(12):1596-602. PMID: 2813200.
56. Lanir Y. Constitutive equations for fibrous connective tissues. *J Biomech*. 1983;16(1):1-12.

57. Bond MD, Van Wart HE. Characterization of the individual collagenases from *Clostridium histolyticum*. *Biochemistry*. 1984;23(13):3085-91.
58. Schnierer S, Kleine T, Gote T, Hillemann A, Knauper V, Tschesche H. The recombinant catalytic domain of human neutrophil collagenase lacks type I collagen substrate specificity. *Biochem Biophys Res Commun*. 1993;191(2):319-26.
59. Bond MD, Van Wart HE. Purification and separation of individual collagenases of *Clostridium histolyticum* using red dye ligand chromatography. *Biochemistry*. 1984;23(13):3077-85.
60. Ruberti JW, Hallab NJ. Strain-controlled enzymatic cleavage of collagen in loaded matrix. *Biochem Biophys Res Commun*. 2005;336(2):483-9.
61. Yuan H, Kononov S, Cavalcante FS, Lutchen KR, Ingenito EP, Suki B. Effects of collagenase and elastase on the mechanical properties of lung tissue strips. *J Appl Physiol*. 2000;89(1):3-14.
62. Rowe J, Chen Q, Domire ZJ, McCullough MB, Sieck G, Zhan WZ, et al. Effect of collagen digestion on the passive elastic properties of diaphragm muscle in rat. *Med Eng Phys*. 2010;32(1):90-4. PMID: 2841476.
63. Barbir A, Michalek AJ, Abbott RD, Iatridis JC. Effects of enzymatic digestion on compressive properties of rat intervertebral discs. *J Biomech*. 2010;43(6):1067-73. PMID: 3004476.
64. Denny E, Schroter RC. Relationships between alveolar size and fibre distribution in a mammalian lung alveolar duct model. *J Biomech Eng*. 1997;119(3):289-97.
65. Komatsu K, Kanazashi M, Arai T, Chiba M. Effects of hydrocortisone and beta-aminopropionitrile on stress-strain and stress-relaxation behaviors, and birefringent retardation of collagen fibers in the rat incisor periodontal ligament. *Connect Tissue Res*. 2002;43(4):581-8.
66. Woessner JF, Jr., Ryan JN. Collagenase activity in homogenates of the involuting rat uterus. *Biochim Biophys Acta*. 1973;309(2):397-405.
67. Clarkson MR, Murphy M, Gupta S, Lambe T, Mackenzie HS, Godson C, et al. High glucose-altered gene expression in mesangial cells. Actin-regulatory protein gene expression is triggered by oxidative stress and cytoskeletal disassembly. *J Biol Chem*. 2002;277(12):9707-12.
68. Reddy GK. Glucose-mediated in vitro glycation modulates biomechanical integrity of the soft tissues but not hard tissues. *J Orthop Res*. 2003;21(4):738-43.
69. Xiu KH, Feola A, Abramowitch, Li ZM. Tensile properties of the transverse carpal ligament in bi-directions. The Cutting Edge together with the 7th Triennial International Hand and Wrist Biomechanics Symposium. Cleveland, OH.

70. Bheyta M. Optimization of enzyme dissociation process based on reaction diffusion model to predict time of tissue digestion. Ph.D. Dissertation, Department of Chemical Engineering, Ohio State University; 2006.
71. Hoffman AH, Ribochaud II DR, Duquette JJ, Grigg P. Determining the effect of hydration upon the properties of the ligaments using pseudo Gaussian stress stimuli. *J Biomech.* 2005;38(8): 1636-42.